ARCHIVES OF MECHANICS
Arch. Mech. **76** (1-2), 155–189, 2024, DOI: 10.24423/aom.4498

Analytical model of a composite girder with flexible adhesive bondline

P. SZEPTYŃSKI

Division of Structural Mechanics and Material Mechanics,
Cracow University of Technology, 24 Warszawska St., 31-155 Krakow, Poland,
e-mail: pawel.szeptynski@pk.edu.pl

The paper presents a linear elastic one-dimensional Discrete Layer–Wise (DLW) analytical model of a composite girder consisting of two beams bonded together with a layer of a flexible adhesive. The model takes into account both longitudinal and transverse deformation of component beams, the First Order Shear Deformation Theory (FSDT) for these adherends as well as extensibility of the adhesive layer. A system of governing equations is derived and a general solution is found with the use of the method of generalized eigenvectors. Two examples are analyzed both with the use of the considered 1D analytical model and a 3D Finite Element Analysis (FEA) in order to validate predictions of the introduced theory. Satisfactory agreement is found between theoretical and numerical results.

Key words: composite girders, adhesive bonding, analytical modelling, closed-form solution, linear elasticity.

1. Introduction

One of the most crucial aspects of designing of composite structures is the problem of providing an appropriate connection between the component parts of such a complex system. Adhesive bonding emerges as one the most promising solutions. Adhesive bondlines have a recommendable strength-to-weight ratio and enable joining almost any pair of materials without a necessity of drilling holes for connectors, what reduces the load-carrying capacity of adherends. They exhibit considerable resistance against corrosion and influences of some chemically aggressive environments. Furthermore, the adhesives themselves may protect structural elements against corrosion and may be used as sealants. For these reasons adhesive bonding is commonly used in the automotive and aerospace industry [1], however, most of these applications do not concern the connection of load-carrying structural elements but rather attaching finishing parts or elements of secondary importance. Adhesive bonding is technologically demanding and requires skilled staff and careful preparation of joined surfaces [2]. Relatively long-lasting curation makes it also more time-consuming technology,

compared to the use mechanical connectors, welding etc. Each adhesive has also only a limited range of allowable service temperatures. Also moisture affects the performance of the joint. The influence of these two factors is discussed e.g. in [3–6]. They may also be vulnerable to the ultraviolet radiation [7, 8] and action of certain chemicals, see e.g. [9, 10]. Adhesive joints are relatively larger then alternative solutions, flaw detection in adhesives is difficult and there are practically no possibilities of repairing the joint. Perhaps the most important reason for which adhesive bonding is not so common in load-carrying structures is that our knowledge on the long-term influence of environmental factors such as temperature, humidity, sunlight exposure etc. is still limited, despite ongoing research [11, 12]. The lack of unambiguous and reliable recommendations makes it risky for designers to evaluate durability of the designed adhesive joint.

This is clearly visible in civil engineering – while there is a great variety of adhesives of different properties provided by manufacturers, most of the connections in buildings are made by ensuring locked contact (e.g. masonry, woodworking joints), by welding, with the use of e.g. bolts, screws, dowels (steel structures) or plate connectors, or they are simply avoided by casting a monolithic structure (concrete structures). Adhesive joints are more commonly used in connecting finishing layers such as glass façade attached to steel substructure [13, 14]. Repair, refurbishment and strengthening are other examples of application of adhesive bonding, especially regarding the objects of cultural heritage. Strengthening of timber structures with adhesively bonded Fiber Reinforced Polymers (FRP) is discussed in [15]. A general review on the use of adhesives in strengthening of masonry structures may be found in [16]. In [17] a technology of repair of a debonded composite strengthening of a masonry structure is presented. The use of flexible polymer joints for improving damping properties of a damaged masonry structure was described in [18]. Adhesive bonding is also a common technique of strengthening of reinforced-concrete (RC) structures [19]. It can be also used to bond cracked concrete together [20] or to attach a new concrete structure to the old one [21].

As regards the important load-carrying joints, it seems that only adhesively bonded rebars and anchors are in common use in engineering practice. This concerns not only RC structures, but also e.g. timber structures [22, 23]. These are also timber structures for which building standards account for gluing technologies – this concern primarily the use of Glue Laminated Timber (GLT), Laminated Veneer Lumber (LVL) or plywood considered as a structural material, but also construction of mechanically jointed beams (EN 1995-1-1, Section B.1.2) as well as spaced columns (Section C.3.1) and lattice columns (Section C.4) by employing adhesive joints. Requirements for phenolic and aminoplastic adhesives used in load-carrying sections of timber structures are given in EN 301 standard, related with EN 1995. It seems, however, that there is still a lack of standards

dealing with a great variety of alternative adhesive types provided by manufacturers, based on i.e. epoxies, polyurethanes, methacrylates, cyanoacrylates. On the other hand, building codes standardizing the construction of reinforced-concrete (EN 1992-1-1), steel (EN 1993-1-8) and composite steel-RC structures (EN 1994-2) do not support design of adhesive joints. It is also beyond the scope of the technical specification CEN/TS 19103 dealing with composite timber-concrete structures.

Nevertheless, adhesive bonding in civil engineering is still a subject of an intense ongoing research [24–27]. In particular, this technology may find multiple applications in the construction of composite structures such as multilayer beams, girders or bridge decks. At present, due to the lack of appropriate building standards, a regular approach is to use stiff mechanical connectors, ensuring complete transmission of displacement between components of the composite element (see Fig. 1). However, employing an adhesive layer as a connector gains popularity, especially when FRP decks are utilized [28–32]. One of the reasons for that is that a surface adhesive bonding enable distribution of stresses over a wider area, as opposed to local concentration of stresses in the neighborhood of connectors. Thin layers of stiff (e.g. epoxy) adhesive provide a rigid connection resulting in similar characteristic of a composite cross-section as in the case of the use of mechanical connectors. However, such stiff adhesives tend to concentrate stress near the ends of a bondline, as it is predicted even by the simplest theories of Volkersen and de Bruyne [33, 34] and supported by the experimental evidence [35, 36]. Contrary to that, employing more compliant (flexible, extensible) connection in the form of a relatively thick layer of an adhesive of low stiffness results in more uniform stress distribution along a bondline [35–37], however, also a significant relative horizontal displacement of components occurs due to shearing of an adhesive layer (Fig. 1). While such a solution apparently may lead to the loss of flexural rigidity of a composite structure, such a conclusion is not

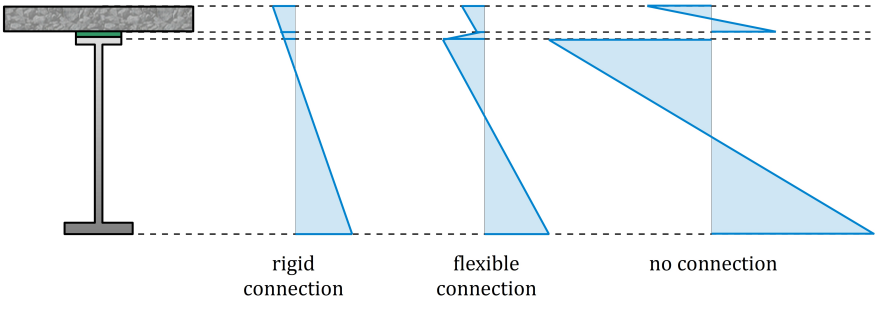

Fig. 1. Strain distribution in a composite cross-section depending on the rigidity of connection between components.

always true [38]. It was shown in [39] that the use of the flexible adhesive provides a residual load-carrying capacity of a cracked RC slab up to 40% greater than the one obtained with the use of the stiff adhesive.

There are multiple mathematical models of composite or multilayer beams, which may be employed for the description of deformation and stress distribution in composite beams and plates. These include the Discrete Layer–Wise (DLW) theories [40, 41] (including zig-zag models [42]) as well as Equivalent Single Layer (ESL) theories [43]. A proposition of an analytical model, closely related to a more general theory presented in [44], was introduced in [45, 46]. This model – based on assumptions of the linear theory of elasticity – deals with multilayer beams consisting of bent layers and sheared adhesive layers placed in an alternating way. Each of the bent layers is considered the Bernoulli–Euler beam and it is assumed that the sheared layer undergoes only simple shear, determined by displacements of the neighboring bent layer at interface with an adhesive. The discussed model emerges to be in good agreement both with experimental results [45] and simulations performed with the use of the Finite Element Method (FEM) [45–47]. Also analytical formulas were derived for maximal deflection, extremal normal stresses in bent layers and extremal shear stress in an adhesive layer [47, 48]. Recently, the model have been employed in a control theory problem optimizing a shape of a composite bridge girder [49]. The major drawback of the presented theory is neglecting the extensibility (longitudinal deformation) of the adhesive layers. In [48] predictions of a number of distinct theories describing the stress distribution in sheared single-lap joint [50–53] were compared with the results of the Finite Element Analysis (FEA). It was shown that accounting for extensibility of an adhesive layer – as in the proposition of Delale, Erdogan and Aydınoglu [51] – is crucial for a correct description of distribution of the peel stress, which is one of the leading factors determining the strength of a joint (see Fig. 2).

For this reason in the current research an attempt is made to generalize the model presented in [45, 46], so that it accounted for longitudinal deformation of an adhesive layer. Also the First Order Shear Deformation Theory (FSDT) is employed by modelling the bent layers within the Timoshenko–Ehrenfest beam theory [54]. Three-layer girders (top beam + adhesive layer + bottom beam) are considered only, since the research is meant to contribute to the problem of modelling of adhesively bonded composite girders and bridge decks. The most important goals achieved in the research and presented in the article are given below:

- A system of governing equations for the problem of plane bending of a composite girder with a flexible adhesive bondline is derived.
- An analytical solution to the problem is found with the use of the method of generalized eigenvectors. A general solution is found as a sum of a gen-

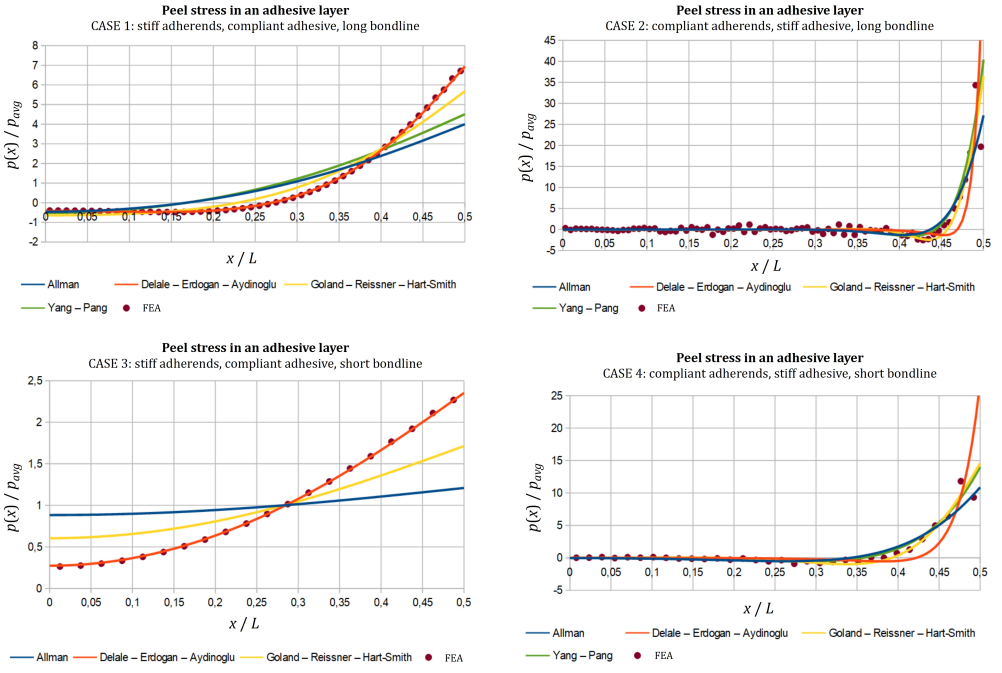

FIG. 2. Peel stress distribution in an adhesive layer in a sheared single-lap joint [48].

eral solution of a homogeneous system of equations and chosen particular solution of a non-homogeneous system. Closed-form formulas are derived for the vectors determining these solutions.

- Two numerical examples are analyzed to validate the theoretical predictions with the results of the FEA. In the first one, a symmetric simply-supported composite RC-steel bridge deck subject to self-weight and uniformly distributed load is considered. In the second example, a simply-supported RC beam strengthened with an adhesively bonded CFRP film subject to four-point bending is analyzed.

2. Model assumptions and derivation of governing equations

We shall deal with a composite girder consisting of two beams bonded together with a layer of a flexible adhesive, as shown in Fig. 3.

The picture shows a typical RC-steel composite girder, however, the presented theory may be applied to any geometry and materials which satisfy the following assumptions:

- The model falls within the framework of the linear theory of elasticity, therefore it is assumed that:

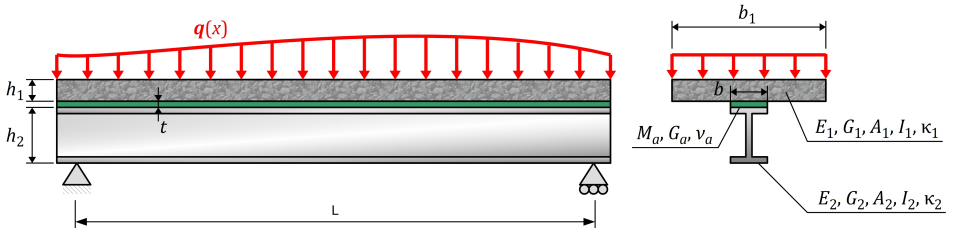

FIG. 3. Composite girder.

  - displacements are small – no second order effects, such as $P-\delta$ or $P-\Delta$ effects, are accounted for,
  - strains are small – the kinematic relations between strains and derivatives of displacements are linear,
  - the material is linear elastic – for each of the materials, the constitutive relation between strains and stresses take the form of linear Hooke's law.
- The beam is only in-plane loaded and only in-plane deformation is considered – out-of-plane buckling or lateral torsional buckling are beyond the scope of the presented theory.
- The beams are slender enough so that their deformation may be properly described with the use of the Timoshenko–Ehrenfest beam theory (Fig. 4).
- The beams exhibit significantly greater longitudinal and transverse rigidity than the adhesive. Under such an assumption it is possible to determine an approximate plane strain state in the adhesive according solely to displacements of the neighboring beams at interfaces with the adhesive layer.

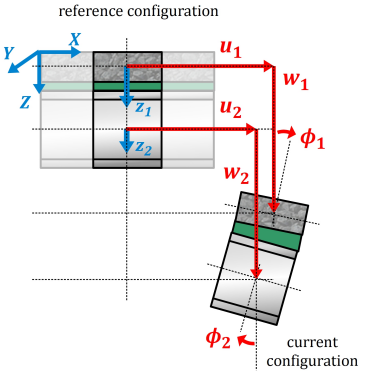

FIG. 4. State variables.

A procedure of derivation of governing equations is analogous to those applied in most of analytical models dealing with adhesively bonded elements,

particularly these presented in [45, 52], where the equations are formulated in terms of generalized displacements and their derivatives. Equations of equilibrium of cross-sectional forces (defined as components of resultant force and resultant moment of a continuous distribution of stresses in a given cross-section) are written down for each of two component beams. Then constitutive relations are employed in order to express the cross-sectional forces in terms of strains and finally kinematic relations are utilized, so that only displacements and their derivatives occur in the final form of equilibrium equations.

2.1. Kinematic relations

Kinematics of beams, according the Timoshenko–Ehrenfest (TE) beam theory, is governed by the assumption that any plane cross-section of an undeformed beam remains plane also after deformation, however, it may undergo a rotation by angle ϕ about an axis parallel to the direction of the bending moment vector. Vertical displacements of points belonging to the given cross-section of the i-th beam are considered constant across the entire cross-section and equal $w_i(x)$ $(i = 1, 2)$. Combining the assumptions of the TE theory with a possibility of longitudinal deformation of the beam, horizontal displacement of point (x, z) of the i-th beam may be expressed as follows:

$$u_i^z(x, z_i) = u_i(x) - \phi_i(x) \cdot z_i \qquad (i = 1, 2), \tag{2.1}$$

where u_i is the horizontal displacement of the centroid of the beam's cross-section, while ϕ_i stands for the angle of rotation of this cross-section. The horizontal displacement of the bottom face of the top beam $\left(z_1 = \frac{h_1}{2}\right)$ is thus equal (B in the superscript stands for the "bottom face"):

$$u_1^B = u_1 - \phi_1 \cdot \frac{h_1}{2}, \tag{2.2}$$

while the horizontal displacement of the top face of the bottom beam $\left(z_2 = -\frac{h_2}{2}\right)$ may be expressed in the following way (T in the superscript stands for the "top face"):

$$u_2^T = u_2 + \phi_2 \cdot \frac{h_2}{2}. \tag{2.3}$$

One may notice, that the above relations assume that both beams' sections are symmetrical about horizontal axis, as the distance from the centroid is half the height of the section. This assumption, however, is not necessary – in case of any non-symmetric section, it is enough to substitute in the place of h_i twice the distance between the centroid and the interface with the bondline.

Strains in beams are calculated according to the linear kinematic relations:

$$\varepsilon_{xx,i} = \frac{du_i^z}{dx} = \frac{du_i}{dx} - \frac{d\phi_i}{dx} \cdot z_i \quad (i = 1, 2), \tag{2.4}$$

$$\varepsilon_{xz,i} = \frac{1}{2}\left(\frac{du_i^z}{dz_i} + \frac{dw_i}{dx}\right) = \frac{1}{2}\left(\frac{dw_i}{dx} - \phi_i\right) \quad (i = 1, 2). \tag{2.5}$$

The longitudinal strain in the adhesive is assumed to be equal an average of the strains at interfaces:

$$\varepsilon_{xx,a} = \frac{1}{2}\left(\frac{du_1^B}{dx} + \frac{du_2^T}{dx}\right) = \frac{1}{2}\left[\left(\frac{du_1}{dx} + \frac{du_2}{dx}\right) + \left(\frac{d\phi_2}{dx} \cdot \frac{h_2}{2} - \frac{d\phi_1}{dx} \cdot \frac{h_1}{2}\right)\right]. \tag{2.6}$$

Please, note that this is only an approximation, since a plane deformation with unequal elongations at interfaces of the adhesive necessarily yields a non-uniform through-the-thickness distribution of $\varepsilon_{xx,a}$. The value given by (2.6) is a mean value of the considered strain in the given cross-section. Vertical displacements in the adhesive are assumed to vary linearly through the thickness, so the corresponding transverse linear strain is constant in the given cross-section:

$$\varepsilon_{zz,a} = \frac{w_2 - w_1}{t}, \tag{2.7}$$

where t stands for the thickness of the adhesive layer. Similarly, it is assumed that the horizontal displacement varies linearly between the values at interfaces which are determined by the deformation of neighboring beams. For this reason the shear strain in the adhesive is also considered constant in the given cross-section:

$$\varepsilon_{xz,a} = \frac{u_2^T - u_1^B}{2t} = \frac{1}{2t}\left[(u_2 - u_1) + \left(\phi_2 \cdot \frac{h_2}{2} + \phi_1 \cdot \frac{h_1}{2}\right)\right]. \tag{2.8}$$

2.2. Constitutive relations

Linear constitutive relations of generalized Hooke's law are employed for each component material. Stress state components in the beams are equal:

$$\begin{aligned} \sigma_{xx,i} &= E_i \varepsilon_{xx,i} = E_i\left(\frac{du_i}{dx} - \frac{d\phi_i}{dx} \cdot z_i\right), \\ \sigma_{xz,i} &= 2G_i \varepsilon_{xz,i} = G_i\left(\frac{dw_i}{dx} - \phi_i\right) \quad (i = 1, 2), \end{aligned} \tag{2.9}$$

where E_i and G_i are Young's longitudinal stiffness modulus, and Kirchhoff's modulus of rigidity, respectively, for a material that the i-th beam is made of. Please, note that according to (2.9) the distribution of shear stress is uniform

over the beams' cross-sections, which contradicts the static boundary conditions requiring them to be zero at outer faces. As it is known that the true distribution of shear stress is non-uniform, it is necessary to introduce a shear correction factor κ_i which would yield correct value of the definite integral determining the resultant shear force. After appropriate integration of stresses over the considered cross-sections:

$$N_i = \iint_{A_i} \sigma_{xx,i}\, dA, \quad Q_i = \iint_{A_i} \kappa_i \sigma_{xz,i}\, dA, \quad M_i = \iint_{A_i} \sigma_{xx,i} z_i\, dA \quad (i = 1, 2), \tag{2.10}$$

the constitutive relations between cross-sectional forces and displacements may be written in the following way:

$$N_i = E_i A_i \frac{du_i}{dx}, \quad Q_i = \kappa_i G_i A_i \left(\frac{dw_i}{dx} - \phi_i \right), \quad M_i = -E_i I_i \frac{d\phi_i}{dx} \quad (i = 1, 2), \tag{2.11}$$

where N_i, Q_i, M_i stand for axial force, transverse shear force and bending moment, respectively, while A_i and I_i are the area of the cross-section and second moment of area of the cross-section of the i-th beam, respectively. The use of the Zhuravsky formula [55] enables simple estimation of the shear correction factor in the following form:

$$\kappa_i = \frac{1}{f_{s,i}} = \left[\frac{A_i}{I_i^2} \iint_{A_i} \frac{S_i^2(z_i)}{b_i^2(z_i)}\, dA \right]^{-1}, \tag{2.12}$$

where $f_{s,i}$ is the form factor, $b_i(z_i)$ is the width of the cross-section at coordinate z_i and $S_i(z_i)$ is the first moment of area about the central horizontal axis of this part of cross-section which is placed beyond z_i line. For I-sections and box-sections an approximation $\kappa_i = A_{web,i}/A_i$ may be used [54]. For an arbitrary cross-section the shear correction factor may be determined numerically [56].

As regards the distribution of shear stress in the component beams, the formula (2.9) is far from being precise. Much more accurate estimate may be provided by the aforementioned Zhuravsky formula, according to which, the mean (through-the-width) shear stress is equal

$$\overline{\sigma}_{xz,i}(x, z_i) = \frac{1}{b_i(z_i)} \iint_{A_i(z_i)} \frac{\partial \sigma^B_{xx,i}}{\partial x}\, dA = -\frac{E_i}{b_i(z_i)} \iint_{A_i(z_i)} \frac{d^2\phi_i}{dx^2} \cdot z_i\, dA, \tag{2.13}$$

where $A_i(z_i)$ is a part of the cross-section which is placed beyond a z_i line and $\sigma^B_{xx,i}$ stands for normal stress due to bending only (normal stresses due to axial forces, even distributed nonuniformly along x axis, are still distributed

uniformly over the cross-section and thus do not produce distortional strain and corresponding shear stress). The area $A_i(z_i)$ should be chosen in such a way, that its outer edge corresponds with the traction free boundary, e.g. for $i = 1$ (top beam) the integration should be performed for $A_i(z_i)$ placed above the centroid, otherwise the integration should account for an additional boundary term corresponding with the interface with the bondline, namely, the magnitude of shear stress in the adhesive layer. Similarly, for $i = 2$ (bottom beam) integration should be performed for $A_i(z_i)$ placed below the centroid.

The adhesive is assumed to be in the plane strain state, so the constitutive relation may be written in the form presented below:

$$\sigma_{xx,a} = M_a\left[\varepsilon_{xx,a} + \frac{\nu_a}{1-\nu_a}\varepsilon_{zz,a}\right], \tag{2.14}$$

$$\sigma_{zz,a} = p = M_a\left[\varepsilon_{zz,a} + \frac{\nu_a}{1-\nu_a}\varepsilon_{xx,a}\right], \tag{2.15}$$

$$\sigma_{xz,a} = \tau = 2G_a\varepsilon_{xz,a}, \tag{2.16}$$

where M_a is the P-wave modulus of the adhesive, ν_a is its Poisson's ratio and G_a stands for modulus of rigidity. These three constants are not independent, as they are bound by the following relation:

$$M_a = 2G_a\frac{1-\nu_a}{1-2\nu_a}. \tag{2.17}$$

It is also possible to define the cross-sectional forces for a composite section. Bending moment about an axis parallel to Y-axis and corresponding with a fixed Z_O coordinate is equal:

(2.18)

$$\begin{aligned} M_O &= M_1 + M_2 + N_1(Z_{O,1} - Z_O) + N_2(Z_{O,2} - Z_O) \\ &= -E_1I_1\frac{d\phi_1}{dx} - E_2I_2\frac{d\phi_2}{dx} + E_1A_1\frac{du_1}{dx}(Z_{O,1} - Z_O) + E_2A_2\frac{du_2}{dx}(Z_{O,2} - Z_O), \end{aligned}$$

where $Z_{O,i}$ denotes the global coordinate of the centroid of the cross-section of the i-th beam. For beams of the symmetric cross-section, one should take $Z_{O,1} = \frac{h_1}{2}$, $Z_{O,2} = h_1 + t + \frac{h_2}{2}$. The shear force may be found according to Schwedler's formula:

$$\begin{aligned} Q = \frac{dM_O}{dx} &= \frac{dM_1}{dx} + \frac{dM_2}{dx} + \frac{dN_1}{dx}Z_{O,1} + \frac{dN_2}{dx}Z_{O,2} \\ &= -E_1I_1\frac{d^2\phi_1}{dx^2} - E_2I_2\frac{d^2\phi_2}{dx^2} + E_1A_1\frac{d^2u_1}{dx^2}Z_{O,1} + E_2A_2\frac{d^2u_2}{dx^2}Z_{O,2}. \end{aligned} \tag{2.19}$$

Please, note that the above result is independent of the choice of Z_O. The remaining term including Z_O cancels since the sum of derivatives of axial forces is null, according to the equations of equilibrium, as it is shown in the following section.

2.3. Equilibrium equations

Equilibrium of forces and moment of forces applied to infinitesimal sections of components of the considered composite girder is depicted in Fig. 5.

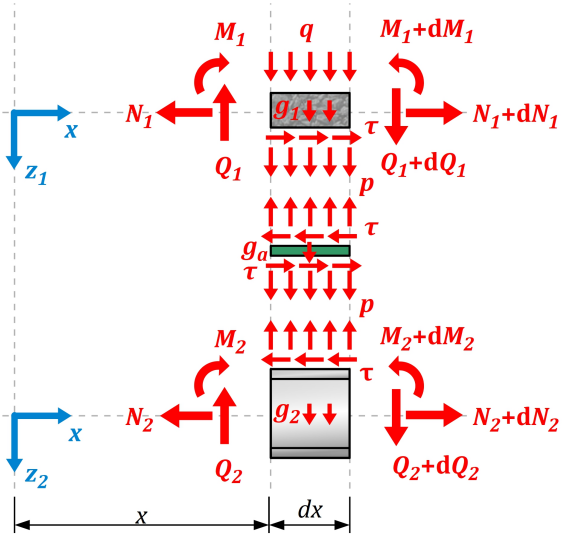

FIG. 5. Equilibrium of external and internal forces applied to a section of a composite girder.

According to this picture, one may write the following equilibrium equations for beams' sections:

$$\frac{dN_1}{dx}+b\tau=0,\quad \frac{dQ_1}{dx}+bp+(b_1q+\gamma_1A_1)=0,\quad \frac{dM_1}{dx}-Q_1+\tau\cdot\frac{bh_1}{2}=0, \tag{2.20}$$

$$\frac{dN_2}{dx}-b\tau=0,\quad \frac{dQ_2}{dx}-bp+\gamma_2A_2=0,\quad \frac{dM_2}{dx}-Q_2+\tau\cdot\frac{bh_2}{2}=0, \tag{2.21}$$

where γ_i is the self-weight of the material that the i-th beam is made of. It is assumed that the shear stress due to shearing of the adhesive acts at the interface, just as it was assumed in e.g. [50, 52, 57–60], contrary to an alternative approach, presented e.g. in [61, 62], in which it was assumed that shear stress is reduced in the middle of the adhesive layer's thickness. After expressing the cross-sectional forces according to (2.11) and substituting (2.6)–(2.8) together with (2.14)–(2.16) we arrive at the following result:

$$
\begin{aligned}
&E_1A_1\frac{d^2u_1}{dx^2}+b\frac{G_a}{t}\left[(u_2-u_1)+\left(\phi_2\cdot\frac{h_2}{2}+\phi_1\cdot\frac{h_1}{2}\right)\right]=0,\\
&E_2A_2\frac{d^2u_2}{dx^2}-b\frac{G_a}{t}\left[(u_2-u_1)+\left(\phi_2\cdot\frac{h_2}{2}+\phi_1\cdot\frac{h_1}{2}\right)\right]=0,
\end{aligned}
\tag{2.22}
$$

$$
\begin{aligned}
&\kappa_1G_1A_1\left(\frac{d^2w_1}{dx^2}-\frac{d\phi_1}{dx}\right)\\
&\quad+bM_a\left[\frac{w_2-w_1}{t}+\frac{\nu_a}{2(1-\nu_a)}\left[\left(\frac{du_1}{dx}+\frac{du_2}{dx}\right)+\left(\frac{d\phi_2}{dx}\cdot\frac{h_2}{2}-\frac{d\phi_1}{dx}\cdot\frac{h_1}{2}\right)\right]\right]\\
&\qquad\qquad+(b_1q+\gamma_1A_1)=0,\\
&\kappa_2G_2A_2\left(\frac{d^2w_2}{dx^2}-\frac{d\phi_2}{dx}\right)\\
&-bM_a\left[\frac{w_2-w_1}{t}+\frac{\nu_a}{2(1-\nu_a)}\left[\left(\frac{du_1}{dx}+\frac{du_2}{dx}\right)+\left(\frac{d\phi_2}{dx}\cdot\frac{h_2}{2}-\frac{d\phi_1}{dx}\cdot\frac{h_1}{2}\right)\right]\right]+\gamma_2A_2=0,\\
&E_1I_1\frac{d^2\phi_1}{dx^2}+\kappa_1G_1A_1\left(\frac{dw_1}{dx}-\phi_1\right)-\frac{bh_1}{2}\frac{G_a}{t}\left[(u_2-u_1)+\left(\phi_2\cdot\frac{h_2}{2}+\phi_1\cdot\frac{h_1}{2}\right)\right]=0,\\
&E_2I_2\frac{d^2\phi_2}{dx^2}+\kappa_2G_2A_2\left(\frac{dw_2}{dx}-\phi_2\right)-\frac{bh_2}{2}\frac{G_a}{t}\left[(u_2-u_1)+\left(\phi_2\cdot\frac{h_2}{2}+\phi_1\cdot\frac{h_1}{2}\right)\right]=0.
\end{aligned}
$$

This is a linear non-homogeneous system of 6 ordinary differential equations (ODEs) of the 2nd order with constant coefficients. It is important to note that the above equilibrium conditions regard the beams only. Local equilibrium in the adhesive is not satisfied, unless:

$$
\begin{cases}
\dfrac{\partial\sigma_{xx,a}}{\partial x}+\dfrac{\partial\sigma_{xz,a}}{\partial z}=0,\\
\dfrac{\partial\sigma_{xz,a}}{\partial x}+\dfrac{\partial\sigma_{zz,a}}{\partial z}+g_abt=0,
\end{cases}
\tag{2.23}
$$

which gives us:

$$
\begin{cases}
\dfrac{1}{2}\left[\left(\dfrac{d^2u_1}{dx^2}+\dfrac{d^2u_2}{dx^2}\right)+\left(\dfrac{d^2\phi_2}{dx^2}\cdot\dfrac{h_2}{2}-\dfrac{d^2\phi_1}{dx^2}\cdot\dfrac{h_1}{2}\right)\right]\\
\qquad\qquad+\dfrac{\nu_a}{1-\nu_a}\dfrac{1}{t}\left(\dfrac{dw_2}{dx}-\dfrac{dw_1}{dx}\right)=0,\\
\dfrac{G_a}{t}\left[\left(\dfrac{du_2}{dx}-\dfrac{du_1}{dx}\right)+\left(\dfrac{d\phi_2}{dx}\cdot\dfrac{h_2}{2}+\dfrac{d\phi_1}{dx}\cdot\dfrac{h_1}{2}\right)\right]+g_abt=0.
\end{cases}
\tag{2.24}
$$

The above equations are not employed in the system of governing equations. Neglecting the equilibrium of stresses in the adhesive layer may be the source of errors in the description of deformation of the adhesive layer, so the distribution of stresses in adhesive should be considered as an approximate one.

The system (2.22) may be written in a much more compact form after introducing non-dimensional variables (please, note that ϕ_i $(i = 1, 2)$ are dimensionless quantities themselves):

$$\xi = \frac{x}{L}, \quad \upsilon_1 = \frac{u_1}{L}, \quad \upsilon_2 = \frac{u_2}{L}, \quad \omega_1 = \frac{w_1}{L}, \quad \omega_2 = \frac{w_2}{L}, \tag{2.25}$$

and non-dimensional similarity numbers:

$$\begin{aligned}
&\pi_{h1} = \frac{h_1}{2L}, \quad \pi_{h2} = \frac{h_2}{2L}, \quad \pi_t = \frac{2L}{t}, \quad \pi_\nu = \frac{\nu_a}{1-\nu_a},\\
&\pi_{q1}(\xi) = \frac{(q(\xi)b_1 + \gamma_1 A_1 g_1)L}{\kappa_1 G_1 A_1}, \quad \pi_{q2} = \frac{\gamma_2 A_2 g_2 L}{\kappa_2 G_2 A_2},\\
&\pi_{N1} = \frac{G_a L^2 b}{E_1 A_1 t}, \qquad \pi_{Q1} = \frac{\kappa_1 G_1 A_1 L^2}{E_1 I_1},\\
&\pi_{M1} = \frac{G_a L^3 b h_1}{2E_1 I_1 t}, \qquad \pi_{a1} = \frac{M_a L b}{2\kappa_1 G_1 A_1},\\
&\pi_{N2} = \frac{G_a L^2 b}{E_2 A_2 t}, \qquad \pi_{Q2} = \frac{\kappa_2 G_2 A_2 L^2}{E_2 I_2},\\
&\pi_{M2} = \frac{G_a L^3 b h_2}{2E_2 I_2 t}, \qquad \pi_{a2} = \frac{M_a L b}{2\kappa_2 G_2 A_2},
\end{aligned} \tag{2.26}$$

where the characteristic length of the problem L maybe chosen in an arbitrary way, e.g. as the girder's spanlength. All these similarity numbers are positive. Then the system (2.22) may be transformed into a linear non-homogeneous system of 12 ODEs of the 1st order with constant coefficients, which may be written down in the following matrix form:

$$\mathbf{y}'(\xi) = \mathbf{A}\mathbf{y}(\xi) + \mathbf{B}(\xi), \tag{2.27}$$

where

$$\mathbf{A} = \begin{bmatrix}
0 & 1 & 0 & 0 & 0 & 0 & 0 & 0 & 0 & 0 & 0 & 0\\
\pi_{N1} & 0 & -\pi_{N1}\pi_{h1} & 0 & 0 & 0 & -\pi_{N1} & 0 & -\pi_{N1}\pi_{h2} & 0 & 0 & 0\\
0 & 0 & 0 & 1 & 0 & 0 & 0 & 0 & 0 & 0 & 0 & 0\\
-\pi_{M1} & 0 & \pi_{M1}\pi_{h1} + \pi_{Q1} & 0 & 0 & -\pi_{Q1} & \pi_{M1} & 0 & \pi_{M1}\pi_{h2} & 0 & 0 & 0\\
0 & 0 & 0 & 0 & 0 & 1 & 0 & 0 & 0 & 0 & 0 & 0\\
0 & -\pi_{a1}\pi_n & 0 & \pi_{a1}\pi_{h1}\pi_n + 1 & \pi_{a1}\pi_t & 0 & 0 & -\pi_{a1}\pi_n & 0 & -\pi_{a1}\pi_{h2}\pi_n & -\pi_{a1}\pi_t & 0\\
0 & 0 & 0 & 0 & 0 & 0 & 0 & 1 & 0 & 0 & 0 & 0\\
-\pi_{N2} & 0 & \pi_{N2}\pi_{h1} & 0 & 0 & 0 & \pi_{N2} & 0 & \pi_{N2}\pi_{h2} & 0 & 0 & 0\\
0 & 0 & 0 & 0 & 0 & 0 & 0 & 0 & 0 & 1 & 0 & 0\\
-\pi_{M2} & 0 & \pi_{M2}\pi_{h1} & 0 & 0 & 0 & \pi_{M2} & 0 & \pi_{M2}\pi_{h2} + \pi_{Q2} & 0 & 0 & -\pi_{Q2}\\
0 & 0 & 0 & 0 & 0 & 0 & 0 & 0 & 0 & 0 & 0 & 1\\
0 & \pi_{a2}\pi_n & 0 & -\pi_{a2}\pi_{h1}\pi_n & -\pi_{a2}\pi_t & 0 & 0 & \pi_{a2}\pi_n & 0 & \pi_{a2}\pi_{h2}\pi_n + 1 & \pi_{a2}\pi_t & 0
\end{bmatrix},$$

$$\mathbf{B}(\xi) = [0,0,0,0,0,-\pi_{q1}(\xi),0,0,0,0,0,-\pi_{q2}(\xi)]^T,$$
$$\mathbf{y}(\xi) = \left[\upsilon_1, \frac{d\upsilon_1}{d\xi}, \phi_1, \frac{d\phi_1}{d\xi}\omega_1, \frac{d\omega_1}{d\xi}, \upsilon_2, \frac{d\upsilon_2}{d\xi}, \phi_2, \frac{d\phi_2}{d\xi}\omega_2, \frac{d\omega_2}{d\xi}\right]^T.$$

Since the considered system of equations is linear, its general solution will be a sum of a general solution of a homogeneous system $\mathbf{y}_H$ and any particular solution of an non-homogeneous system $\mathbf{y}_N$:

$$\mathbf{y} = \mathbf{y}_H + \mathbf{y}_N. \tag{2.28}$$

3. Closed-form analytical solution of the system of governing equations

3.1. Generalized eigenvectors

The matrix of coefficients $\mathbf{A}$ in (2.27) is a non-diagonalizable matrix. Geometric multiplicity of some of its eigenvalues is less than their algebraic multiplicity, which means that there are less linearly independent eigenvectors corresponding with repeated eigenvalues than the multiplicity of this eigenvalues as a root of a characteristic polynomial. As a result the set of regular eigenvectors only is not large enough to form a fundamental solution, namely a basis of a vector space of solutions to this system. Such problems may be solved with the use of the method of generalized eigenvectors [46, 63, 64].

It may be checked that $\lambda_1 = 0$ is a repeated eigenvalue of $\mathbf{A}$ of algebraic multiplicity $k_1 = 6$, however, there are only $m_1 = 2$ linearly independent eigenvectors corresponding with λ_1:

$$\begin{aligned}\mathbf{v}_{1,1,1} &= [1,\ 0,\ 0,\ 0,\ 0,\ 0,\ 1,\ 0,\ 0,\ 0,\ 0,\ 0]^T,\\ \mathbf{v}_{1,2,1} &= [0,\ 0,\ 0,\ 0,\ 1,\ 0,\ 0,\ 0,\ 0,\ 0,\ 1,\ 0]^T.\end{aligned} \tag{3.1}$$

An indeterminate system of equations for components of a generalized eigenvector $\mathbf{v}$ is considered:

$$(\mathbf{A} - \lambda_1\mathbf{I})^{k_1 - m_1 + 1}\mathbf{v} = \mathbf{0}, \tag{3.2}$$

where $\mathbf{I}$ is a 12×12 unit matrix. Within a six-parameter family of solutions of the above system, two linearly independent solutions were found – a generalized eigenvector $\mathbf{v}_{1,1,2}$ of rank $r_1 = 2$, and a generalized eigenvector $\mathbf{v}_{1,2,4}$ of rank $r_2 = 4$ such that:

$$(\mathbf{A} - \lambda_i\mathbf{I})^{r_j - 1}\mathbf{v}_{k,j,r_j} \neq \mathbf{0} \ \wedge\ (\mathbf{A} - \lambda_i\mathbf{I})^{r_j}\mathbf{v}_{k,j,r_j} = \mathbf{0}. \tag{3.3}$$

The two found vectors generate two linearly independent chains of generalized eigenvectors according to the general formula:

$$\mathbf{v}_{k,j,s} = (\mathbf{A} - \lambda_i\mathbf{I})^{r_j - s}\mathbf{v}_{k,j,r_j} \quad (k = 1,\ j = 1,2,\ s = 1,\ldots,r_j). \tag{3.4}$$

A collection of the generalized eigenvectors of $\mathbf{A}$ is then as follows:

$$\mathcal{E} = \left\{ \begin{pmatrix} \mathbf{v}_{1,1,1} \\ \mathbf{v}_{1,1,2} \end{pmatrix} \begin{pmatrix} \mathbf{v}_{1,2,1} \\ \mathbf{v}_{1,2,2} \\ \mathbf{v}_{1,2,3} \\ \mathbf{v}_{1,2,4} \end{pmatrix} \right\}, \tag{3.5}$$

where the chains of the generalized eigenvectors may be expressed in the following way

$$\begin{pmatrix} \mathbf{y_1} = \mathbf{v}_{1,1,1} = [1,\ 0,\ 0,\ 0,\ 0,\ 0,\ 1,\ 0,\ 0,\ 0,\ 0,\ 0]^T \\ \mathbf{y_2} = \mathbf{v}_{1,1,2} = [0,\ 1,\ 0,\ 0, \alpha_0,\ 0,\ 0,\ 1,\ 0,\ 0,\ 0,\ 0]^T \end{pmatrix}, \tag{3.6}$$

$$\begin{pmatrix} \mathbf{y_3} = \mathbf{v}_{1,2,1} = [0,\ 0,\ 0,\ 0,\ 1,\ 0,\ 0,\ 0,\ 0,\ 0,\ 1,\ 0]^T \\ \mathbf{y_4} = \mathbf{v}_{1,2,2} = [\alpha_1,\ 0,\ 1,\ 0,\ 0,\ 1,\ \alpha_2,\ 0,\ 1,\ 0,\ 0,\ 1]^T \\ \mathbf{y_5} = \mathbf{v}_{1,2,3} = [0,\ \alpha_1,\ 0,\ 1,\ \alpha_3,\ 0,\ 0,\ \alpha_2,\ 0,\ 1,\ \alpha_4,\ 0]^T \\ \mathbf{y_6} = \mathbf{v}_{1,2,4} = [\alpha_5\ 0\ \alpha_6\ 0\ 0\ \alpha_3\ 0\ 0\ -\alpha_6\ 0\ 0\ \alpha_4]^T \end{pmatrix}, \tag{3.7}$$

where

$$\begin{aligned}
&\alpha_0 = \frac{2\pi_\nu}{\pi_t}, \quad \alpha_1 = \pi_{N1}\frac{\beta_{h1}}{\beta_N}, \quad \alpha_2 = -\pi_{N2}\frac{\beta_{h1}}{\beta_N}, \\
&\alpha_3 = -\beta_1 + \beta_3, \quad \alpha_4 = -\beta_1 - \beta_3, \quad \alpha_5 = -\beta_4 - \beta_5, \quad \alpha_6 = \beta_2 + \beta_3, \\
&\beta_1 = \frac{\beta_S\beta_{h1} + \beta_N\beta_Q}{2\pi_{Q1}\pi_{Q2}\beta_N}, \quad \beta_2 = \frac{\beta_T\beta_{h1} + \beta_N\beta_R}{2\pi_{Q1}\pi_{Q2}\beta_N}, \quad \beta_3 = \frac{\pi_\nu\beta_M}{\pi_t\beta_N}, \\
&\beta_4 = \frac{\beta_T\beta_{h4} + \beta_N\beta_R\beta_{h2} - 2\pi_{Q1}\pi_{Q2}\beta_{h1}}{2\pi_{Q1}\pi_{Q2}\beta_N}, \quad \beta_5 = \frac{\pi_\nu\beta_{h2}\beta_M}{\pi_t\beta_N}, \\
&\beta_S = \pi_{M1}\pi_{Q2} + \pi_{M2}\pi_{Q1}, \quad \beta_T = \pi_{M1}\pi_{Q2} - \pi_{M2}\pi_{Q1}, \\
&\beta_M = \pi_{N1}\pi_{h2} - \pi_{N2}\pi_{h1}, \quad \beta_N = \pi_{N1} + \pi_{N2}, \\
&\beta_Q = \pi_{Q1} + \pi_{Q2}, \quad \beta_R = \pi_{Q2} - \pi_{Q1}, \\
&\beta_{h1} = \pi_{h1} + \pi_{h2}, \quad \beta_{h2} = \pi_{h2} - \pi_{h1}, \\
&\beta_{h3} = \pi_{h1}^2 + \pi_{h2}^2, \quad \beta_{h4} = \pi_{h2}^2 - \pi_{h1}^2.
\end{aligned}$$

Total number of generalized eigenvectors stored in the collection $\mathcal{E}$ is 6, which is equal to k_1 – this means that the considered collection is complete.

The rest of eigenvalues λ of matrix $\mathbf{A}$ may be found as the non-zero roots of a characteristic polynomial $\det(\mathbf{A} - \lambda\mathbf{I}) = 0$. This is an even polynomial of degree 6 of the following form:

$$e(\lambda) = \lambda^6 + J_4\lambda^4 + J_2\lambda^2 + J_0 = 0, \tag{3.8}$$

where

$$
\begin{aligned}
J_0 &= -\beta_P \pi_t, \\
\beta_P &= \beta_{h1}(\pi_{M1}\pi_{Q2}\pi_{a2} + \pi_{M2}\pi_{Q1}\pi_{a1}) + \beta_N(\pi_{Q1}\pi_{a1} + \pi_{Q2}\pi_{a2}), \\
J_2 &= \pi_t((\pi_{a1} + \pi_{a2})(\pi_{h1}\pi_{M1} + \pi_{h2}\pi_{M2} + \beta_N) + (\pi_{Q1}\pi_{a1} + \pi_{Q2}\pi_{a2})) \\
&\quad - 2\pi_\nu(\pi_{h1}\pi_{h2}(\pi_{M1}\pi_{Q2}\pi_{a2} + \pi_{M2}\pi_{Q1}\pi_{a1}) \\
&\quad + (\pi_{h1}\pi_{Q1}\pi_{a1}\pi_{N2} + \pi_{h2}\pi_{Q2}\pi_{a2}\pi_{N1})), \\
J_4 &= \pi_\nu(\pi_{h1}\pi_{Q1}\pi_{a1} + \pi_{h2}\pi_{Q2}\pi_{a2}) - \pi_t(\pi_{a1} + \pi_{a2}) - (\pi_{h1}\pi_{M1} + \pi_{h2}\pi_{M2}) - \beta_N.
\end{aligned}
$$

After substituting $X = \lambda^2$ the equation becomes cubic and its roots may be found with the use of any of classical methods [65]. Cubic equations may have either three real roots or one real and two complex conjugate roots. A simplified numerical analysis indicates that within the range of most commonly used values of similarity numbers, occurrence of either of these two cases depends primarily on the stiffness of the adhesive layer. For flexible bondline (compliant material, relatively large thickness of the adhesive layer) there are usually 2 real opposite eigenvalues and four eigenvalues which are square roots of two complex conjugate numbers; for stiff adhesives and thin adhesive layers there are usually 6 real pairwise opposite roots. One should be aware, however, that these observations may fail for a particular set of similarity numbers as other root configurations are also possible – while for any positive similarity numbers J_0 is always negative, no unambiguous conclusion may be derived from this assumption as regards the remaining two coefficients. As a result any combination of real and complex, positive or negative roots is possible for the cubic equation and thus multiple possible sets of real and complex roots may occur for the original sextic equation.

Once the eigenvalue is determined, the corresponding eigenvector may be determined as a solution of an indeterminate system of linear equations after assuming any fixed (non-zero) value of a number of unknown components of this vector – this number, according to the Kronecker–Capelli theorem, is equal the difference between the number of components of the vector and the rank of matrix of coefficients of the considered system of equations. An analytical closed-form expressions may be found for the components of the eigenvectors corresponding with non-zero eigenvalues, they are, however, rather lengthy and cumbersome.

3.2. General solution of a homogeneous system

The part of the general solution of the homogeneous system

$$\mathbf{y}'_H(\xi) = \mathbf{A}\mathbf{y}_H(\xi), \tag{3.9}$$

corresponding with the repeated eigenvalue $\lambda_1 = 0$ may be written in the following form:

$$\mathbf{y}_{H,1}(\xi) = C_1\mathbf{y_1} + C_2(\xi\mathbf{y_1} + \mathbf{y_2}) + C_3\mathbf{y_3} + C_4(\xi\mathbf{y_3} + \mathbf{y_4}) + C_5\left(\frac{\xi^2}{2}\mathbf{y_3} + \xi\mathbf{y_4} + \mathbf{y_5}\right) + C_6\left(\frac{\xi^3}{6}\mathbf{y_3} + \frac{\xi^2}{2}\mathbf{y_4} + \xi\mathbf{y_5} + \mathbf{y_6}\right). \tag{3.10}$$

The form of the remaining part of the general solution depends on whether the eigenvalue corresponding with a basis solution is real or complex. For real eigenvalues λ_k and related eigenvectors $\mathbf{v}_k$ the corresponding solution is equal:

$$\mathbf{y}_{H,k}(\xi) = e^{\lambda_k \xi}\mathbf{v}_k, \tag{3.11}$$

while in the case of a pair of conjugate complex eigenvalues $\lambda_k = \rho_k + i \cdot \theta_k$ and $\lambda_{k+1} = \overline{\lambda_k} = \rho_k - i \cdot \theta_k$ and related eigenvectors $\mathbf{v}_k$ and $\mathbf{v}_{k+1} = \overline{\mathbf{v}_k}$ we have:

$$\mathbf{y}_{H,k}(\xi) = e^{\rho_k \xi}[C_k(\cos(\theta_k\xi) \cdot \Re(\mathbf{v}_k) - \sin(\theta_k\xi) \cdot \Im(\mathbf{v}_k)) + C_{k+1}(\cos(\theta_k\xi) \cdot \Im(\mathbf{v}_k) + \sin(\theta_k\xi) \cdot \Re(\mathbf{v}_k))]. \tag{3.12}$$

Constants of integration C_k $(k = 1, \ldots, 12)$ should be determined according to the prescribed boundary conditions describing either the kinematic constraints imposed on displacements of the girder or static loads applied to the end cross-sections or compatibility and equilibrium conditions in cross-sections loaded in a pointwise manner.

3.3. Particular solution of a non-homogeneous system

If the vector $\mathbf{B}(\xi) \neq 0$, the system becomes non-homogeneous. Non-zero $\mathbf{B}$ corresponds with external load applied to the beam in the form of body forces or distributed surface tractions given by the function $q(x)$ [N/m^2]. One of the most common case of external load is the uniformly distributed load (UDL) given by $q(x) = q = \text{const}$. It corresponds also with a uniformly distributed self-weight. Such a function is a specific case of a quasi-polynomial function:

$$\mathbf{B}(\xi) = e^{\eta\xi} \cdot \sum_{i=0}^{K} \mathbf{B}_i \xi^i. \tag{3.13}$$

For UDL we have $\eta = 0$ and $K = 0$. A particular solution to the non-homogeneous problem is also expected in the form of a quasi-polynomial function:

$$\mathbf{y}_N(\xi) = e^{\eta\xi} \cdot \sum_{i=0}^{L} \mathbf{D}_i \xi^i. \tag{3.14}$$

If the exponent η is distinct from eigenvalues of $\mathbf{A}$, then the degree L is expected to be equal to K. Otherwise, it needs to be augmented with the length of the longest Jordan chain, which in our case is equal to 4 (see: Eq. 3.5). In

the case of UDL we have $\eta = \lambda_1 = 0$, so $L = K + 4 = 4$. We shall consider two cases corresponding with similarity numbers π_{q1} and π_{q2}, which – due to linearity of the system – may be superimposed. In both cases the general form of the particular solution depending on 30 unknown coefficients $a_{i,j}$ ($i = 1, \ldots, 6$; $j = 0, \ldots, 4$) is assumed as follows:

$$\mathbf{y_N} = [y_{N,1}, y_{N,2}, y_{N,3}, y_{N,4}, y_{N,5}, y_{N,6}, y_{N,7}, y_{N,8}, y_{N,9}, y_{N,10}, y_{N,11}, y_{N,12}]^T, \tag{3.15}$$

where

$$y_{N,(2i-1)} = a_{i,0} + a_{i,1}\xi + a_{i,2}\xi^2 + a_{i,3}\xi^3 + a_{i,4}\xi^4, \quad y_{N,2i} = \frac{d}{d\xi} y_{N,(2i-1)}, \quad i = 1, \ldots, 6.$$

After substituting (3.15) in (2.27) we obtain an indeterminate linear system of equations for coefficients $a_{i,j}$. A six-parameter family of solutions may be found. Any particular solution may be taken in order to construct a general solution of (2.27).

CASE 1. $\pi_{q1} \neq 0$ and $\pi_{q2} = 0$ (surface tractions applied to the top beam and/or self-weight of the top beam). Non-zero coefficients are given by the following relationships:

$$\frac{a_{1,3}}{\pi_{N1}} = -\frac{a_{4,3}}{\pi_{N2}} = \frac{\pi_{q1}}{6\beta_P}(\pi_{Q1}\pi_{Q2}\pi_{a2}\beta_{h1}),$$

$$a_{2,3} = a_{5,3} = 4a_{3,4} = 4a_{6,4} = \frac{\pi_{q1}}{6\beta_P}(\pi_{Q1}\pi_{Q2}\pi_{a2}\beta_N),$$

$$a_{3,2} = -\frac{\pi_{q1}}{2\beta_P}(\pi_{Q2}\pi_{a2}(\pi_{M1}\beta_{h1} + \beta_N)),$$

$$a_{4,1} = \frac{\pi_{q1}\pi_{a2}}{\pi_t\beta_P}[\pi_t(\pi_{h2}(\beta_T\beta_{h1} + \beta_N\beta_R) - \pi_{Q1}\pi_{Q2}\beta_{h1}) + 2\pi_\nu\pi_{Q1}\pi_{Q2}\pi_{h2}\beta_M],$$

$$a_{5,1} = -\frac{\pi_{q1}\pi_{a2}}{\pi_t\beta_P}[\pi_t(\beta_T\beta_{h1} + \beta_N\beta_R) + 2\pi_\nu\pi_{Q1}\pi_{Q2}\beta_M],$$

$$a_{6,0} = \frac{\pi_{q1}\pi_{Q1}}{\pi_t\beta_P}[\beta_{h1}(\pi_\nu\pi_{Q2}\pi_{a2} - \pi_{M2}) - \beta_N],$$

$$a_{6,2} = -\frac{\pi_{q1}\pi_{a2}}{2\pi_t\beta_P}[\pi_t\pi_{Q2}(\pi_{M1}\beta_{h1} + \beta_N) + 2\pi_\nu\pi_{Q1}\pi_{Q2}\beta_M].$$

CASE 2. $\pi_{q1} = 0$ and $\pi_{q2} \neq 0$ (self-weight of the bottom beam). Non-zero coefficients are given by the following relationships:

$$\frac{a_{1,3}}{\pi_{N1}} = -\frac{a_{4,3}}{\pi_{N2}} = \frac{\pi_{q2}}{6\beta_P}(\pi_{Q1}\pi_{Q2}\pi_{a1}\beta_{h1}),$$

$$a_{2,3} = a_{5,3} = 4a_{3,4} = 4a_{6,4} = \frac{\pi_{q2}}{6\beta_P}(\pi_{Q1}\pi_{Q2}\pi_{a1}\beta_N),$$

$$a_{3,2} = -\frac{\pi_{q2}}{2\beta_P}(\pi_{Q2}\pi_{a1}(\pi_{M1}\beta_{h1} + \beta_N)),$$

$$a_{4,1} = \frac{\pi_{q2}\pi_{a1}}{\pi_t\beta_P}[\pi_t(\pi_{h2}(\beta_T\beta_{h1} + \beta_N\beta_R) - \pi_{Q1}\pi_{Q2}\beta_{h1}) + 2\pi_\nu\pi_{Q1}\pi_{Q2}\pi_{h2}\beta_M],$$
$$a_{5,1} = -\frac{\pi_{q2}\pi_{a1}}{\pi_t\beta_P}[\pi_t(\beta_T\beta_{h1} + \beta_N\beta_R) + 2\pi_\nu\pi_{Q1}\pi_{Q2}\beta_M],$$
$$a_{6,0} = \frac{\pi_{q2}\pi_{Q2}}{\pi_t\beta_P}[\beta_{h1}(\pi_\nu\pi_{Q1}\pi_{a1} + \pi_{M1}) + \beta_N],$$
$$a_{6,2} = -\frac{\pi_{q2}\pi_{a1}}{2\pi_t\beta_P}[\pi_t\pi_{Q2}(\pi_{M1}\beta_{h1} + \beta_N) + 2\pi_\nu\pi_{Q1}\pi_{Q2}\beta_M].$$

Point forces and point moments may be also modelled by taking $q(\xi)$ equal to Dirac's δ distribution or its derivative δ', respectively. They may be also more easily taken into account by splitting the solution into two parts describing the deformation at each of two sides of the point of application of the load and formulating an appropriate system of continuity conditions involving the displacement compatibility conditions as well as the force equilibrium conditions.

4. Numerical validation of the theoretical model

Two cases are studied both analytically and numerically, with the use of Abaqus/CAE 2022 FEA software. The first example is a section of a simply supported composite RC-steel bridge deck in which the top slab is connected with a non-symmetric steel I-beam with the use of a thick and flexible adhesive layer. The girder is subject to body forces and UDL. The second example is a reinforced-concrete simply-supported beam strengthened with a CFRP film attached at the bottom face with the use of a thin and stiff adhesive layer, which – due to its placement – undergoes significant elongation (contrary to the bondline in the first example, which is placed near the section's neutral axis). The beam is subject to four point bending. Material parameters used in these examples are listed in Table 1. As regards the values of Poisson's ratio of the polyurethane adhesives and CFRP, no data is available for these particular materials, which were employed in the examples – they were estimated according to published measurements performed on similar materials.

Since the considered analytical model as well as the numerical one are linear, obtained results may be scaled proportionally to the magnitude of applied load. Deflections and normal stresses are presented as relative values where the reference value is the one corresponding with a composite cross-section satisfying Bernoulli's hypothesis of plane cross-section (strictly rigid connection at interface – see Fig. 1):

$$w_{\mathrm{ref}} = \alpha_k \frac{M_R L^2}{E_R I_R}, \qquad \sigma_{\mathrm{min,ref}} = \frac{E_1}{E_R}\frac{M_R}{I_R}|z_{\min}|,$$
$$\sigma_{\mathrm{max,ref}} = \frac{E_2}{E_R}\frac{M_R}{I_R}|z_{\max}|, \qquad \sigma_{a,\mathrm{ref}} = \frac{E_a}{E_R}\frac{M_R}{I_R}|z_a|, \tag{4.1}$$

TABLE 1. Mechanical properties of materials used in numerical examples.

Young's modulus of a concrete [66]	$E_c = 32.837\,\text{GPa}$
Poisson's ratio of a concrete [66]	$\nu_c = 0.2$
Self-weight of a concrete [66]	$\gamma_c = 25\ \text{kN/m}^3$
Young's modulus of a steel [67]	$E_s = 210\,\text{GPa}$
Poisson's ratio of a steel [67]	$\nu_s = 0.3$
Self-weight of a steel [67]	$\gamma_s = 78.5\,\text{kN/m}^3$
Young's modulus of Sika©CarboDur© S512 [68]	$E_{\text{CFRP}} = 165\,\text{GPa}$
Poisson's ratio of Sika©CarboDur© S512 [69]	$\nu_{\text{CFRP}} = 0.3$
Self-weight of Sika©CarboDur© S512 [68]	$\gamma_{\text{CFRP}} = 16\,\text{kN/m}^3$
Young's modulus of Sika©PS adhesive [47]	$E_{\text{PS}} = 24.10\,\text{MPa}$
Poisson's ratio of Sika©PS adhesive [70, 71]	$\nu_{\text{PS}} = 0.4$
Young's modulus of Sika©PT adhesive [47]	$E_{\text{PT}} = 779.74\,\text{MPa}$
Poisson's ratio of Sika©PT adhesive [70, 71]	$\nu_{\text{PT}} = 0.4$

where M_R stands for the maximum bending moment determined by means of standard methods of structural mechanics, I_R is the weighted 2nd moment of area of the composite cross-section satisfying Bernoulli's hypothesis, and E_R is any reference Young's modulus:

$$I_R = \frac{E_1}{E_R}\left[I_1 + A_1\left(\frac{h_1}{2} - z_R\right)^2\right] + \frac{E_2}{E_R}\left[I_2 + A_2\left(h_1 + t + \frac{h_2}{2} - z_R\right)^2\right] + \frac{E_a}{E_R}\left[\frac{bt^3}{12} + bt\left(h_1 + \frac{t}{2} - z_R\right)^2\right], \tag{4.2}$$

$$z_R = \frac{\frac{E_1}{E_R}A_1\frac{h_1}{2} + \frac{E_2}{E_R}A_2\left(h_1 + t + \frac{h_2}{2}\right) + \frac{E_a}{E_R}bt\left(h_1 + \frac{t}{2}\right)}{\frac{E_1}{E_R}A_1 + \frac{E_2}{E_R}A_2 + \frac{E_a}{E_R}bt}. \tag{4.3}$$

Coordinates $z_{\min}$, $z_{\max}$ and z_a correspond with the distance of top fibers, bottom fibers and centroid of adhesive layer, respectively, from the centroid of the cross-section with rigid connection at interface. In the above formulas, necessary adjustments must be made in case of non-symmetric cross-sections.

Shear stress is related to the following reference value:

$$\tau_{\text{ref}} = \frac{G_a q_e L^3 b(h_1 + h_2)}{4t(E_1 I_1 + E_2 I_2)} \frac{\lambda(e^\lambda + 1) - 2(e^\lambda - 1)}{\lambda^3(e^\lambda + 1)}, \tag{4.4}$$

where

$$\lambda = L\sqrt{G_a \frac{b}{t}\left[\frac{(h_1 + h_2 + 2t)(h_1 + h_2)}{4(E_1 I_1 + E_2 I_2)} + \left(\frac{1}{E_1 A_1} + \frac{1}{E_2 A_2}\right)\right]}. \tag{4.5}$$

This is a theoretical value of maximum shear stress at the end of a simply supported composite girder consisting of two bisymmetric beams connected with an adhesive layer and loaded with UDL q_e, according to a simplified theory in which longitudinal deformation of the adhesive is neglected [48]. For loads other than UDL, the equivalent UDL q_e is taken as the resultant of all vertical loads divided by the surface area of horizontal faces of the adhesive layer:

$$q_e = \frac{\Sigma F_z}{bL}. \tag{4.6}$$

The results obtained from the theoretical model presented in this article (denoted with TM 1) and from the Finite Element Analysis are also compared with theoretical predictions of the simplified model (TM 2) in which longitudinal deformation of the adhesive layer and shear deformation of beams are disregarded [45, 46].

4.1. Example No 1 – composite RC-steel girder under UDL and self-weight

The element under consideration is a repetitive section of a composite bridge deck consisting of a reinforced-concrete slab and a non-symmetric welded thin-walled steel I-section bonded together with a flexible polyurethane Sika©PS adhesive. Geometry of the cross-section is shown in Fig. 6. The deck is subject to UDL of magnitude $5\,\mathrm{kN/m^2}$. Girder's self-weight is applied in the form of the body forces. The beam is simply supported and the span length is equal 16.75 m.

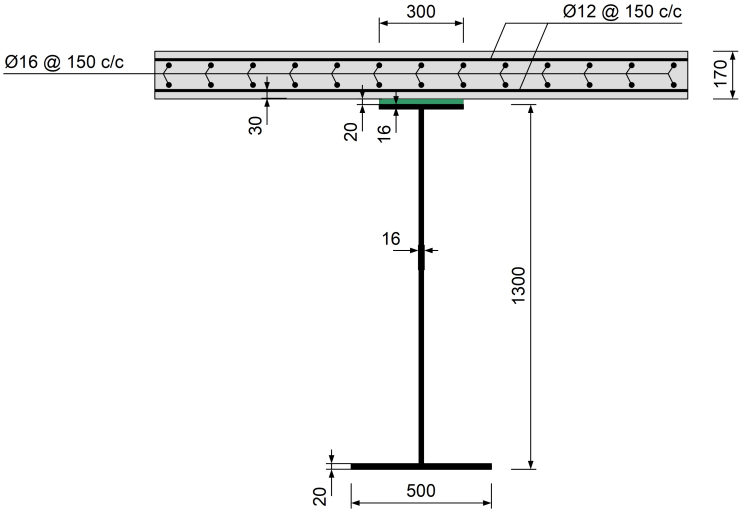

FIG. 6. Cross-section of a section of a composite RC-steel bridge deck.

As regards the analytical model, weighted mechanical characteristics were determined for the RC slab. The solution is given by the sum of general solution

of a homogeneous system and particular solution of non-homogeneous system, since $\pi_{q1} \neq 0$ and $\pi_{q2} \neq 0$. It depends on 12 constants of integration, which are determined with the use of the following boundary condition:

$$\begin{array}{ll} \text{Supported end:} & \text{Middle of the span:} \\ \begin{cases} N_1(0) = 0, \\ N_2(0) = 0, \\ M_1(0) = 0, \\ M_2(0) = 0, \\ w_2(0) = 0, \\ \sigma_{xx,a}(0) = 0, \end{cases} & \begin{cases} u_1(L/2) = 0, \\ u_2(L/2) = 0, \\ Q_1(L/2) = 0, \\ Q_2(L/2) = 0, \\ \phi_1(L/2) = 0, \\ \phi_2(L/2) = 0. \end{cases} \end{array} \tag{4.7}$$

Strictly speaking, it is the bottom beam which is supported, and thus it is required that $w_2(0) = 0$. The deflection of the top slab may be not equal to zero and thus produce compression of the adhesive layer. A more appropriate boundary condition is that normal stress in adhesive is zero at the traction free boundary. However, in the specific case of a simply supported beam, in which both end axial forces and both end bending moments are equal to zero, it may be checked with (2.6) and (2.11) that $\varepsilon_{xx,a} = 0$. As a result, the condition $\sigma_{xx,a}(0) = 0$ is equivalent to $\varepsilon_{zz,a}(0) = 0$ according to (2.13), what yields $\sigma_{zz}(0) = 0$ and – due to (2.7) – also $w_1(0) = w_2(0)$. It is an unrealistic situation, thus the distribution of axial and transverse normal stresses in the adhesive are flawed in this situation, especially in the neighborhood of the traction-free end.

Since the considered analytical model is a linear elastic one, also in the numerical model all materials are assumed to be linear elastic. For this reason cracking of the concrete is disregarded. Reinforcement bars are modelled as truss elements embedded in the volume of the concrete. Interfaces between component beams and adhesive layer were tied one with another due to the use of finer mesh in the adhesive layer. Due to symmetry of the problem only a quarter of the girder was modelled and symmetry boundary conditions were applied (Fig. 7). Symmetry was also assumed at the side face of the concrete slab, as the considered girder is a repetitive section of a wider bridge deck. A support was modelled by constraining vertical displacement on a small region on the bottom face of the steel section.

Graphs presenting distribution of relative values of deflection, normal stresses in edge fibers of component beams as well as shear stress and longitudinal normal stress in the adhesive are presented in Figs. 8–13. Due to symmetry, only half of the graph is presented. The reference values given by (4.1) and (4.4) are calculated with the use of:

$$\alpha_k = \frac{5}{48}, \qquad M_R = \frac{q_{\text{tot}} L^2}{8}, \qquad q_{\text{tot}} = qb_1 + \gamma_1 A_1 + \gamma_2 A_2, \qquad q_e = \frac{q_{\text{tot}}}{b}.$$

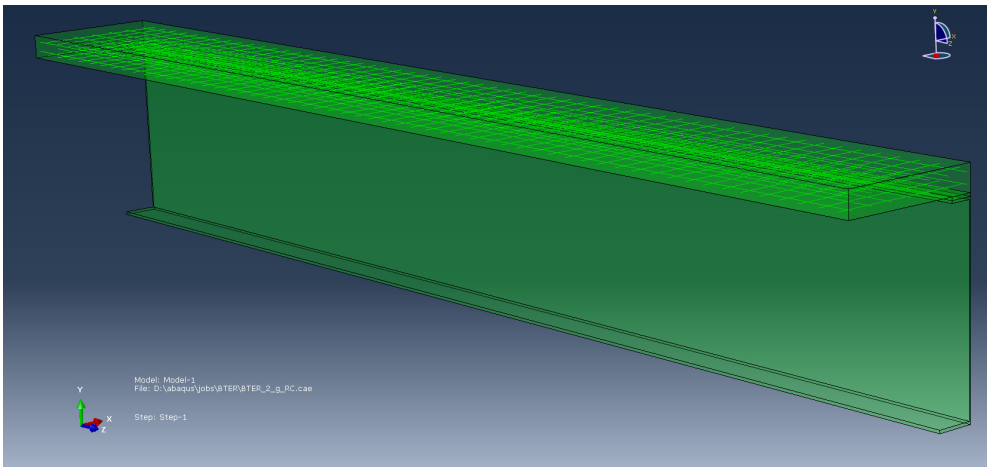

FIG. 7. Numerical model of the composite bridge deck.

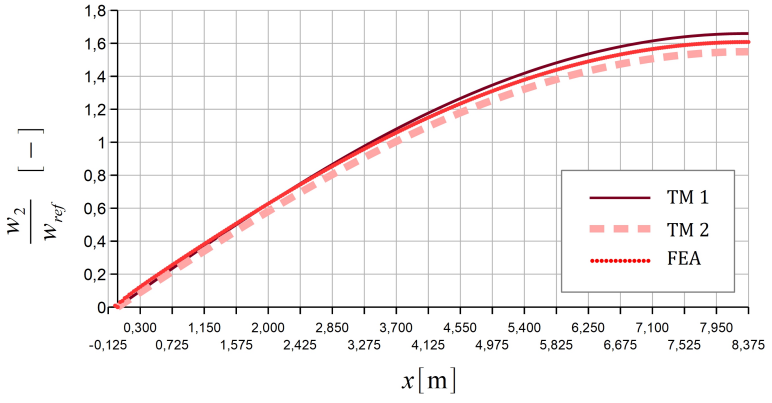

FIG. 8. Deflection of the bottom face of steel I-section.

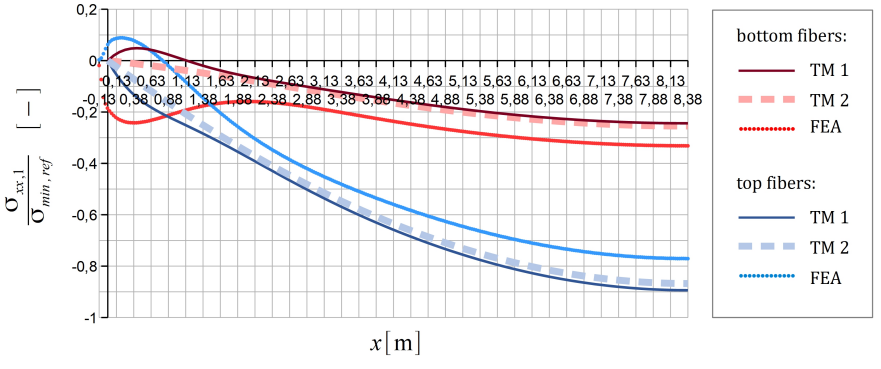

FIG. 9. Normal stress in top and bottom fibers in the RC slab.

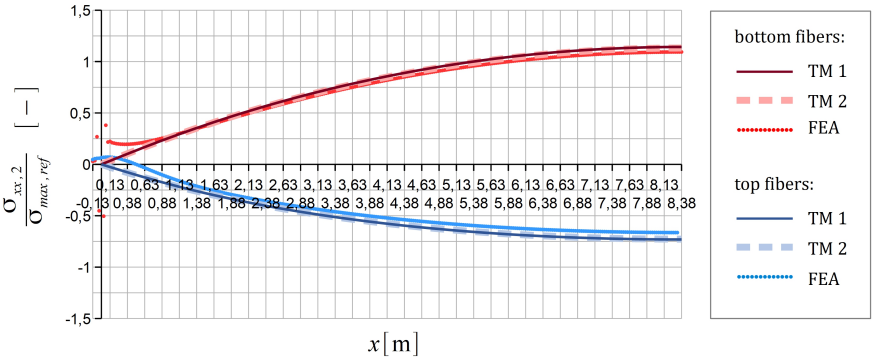

FIG. 10. Normal stress in the top and bottom fibers of the steel I-section.

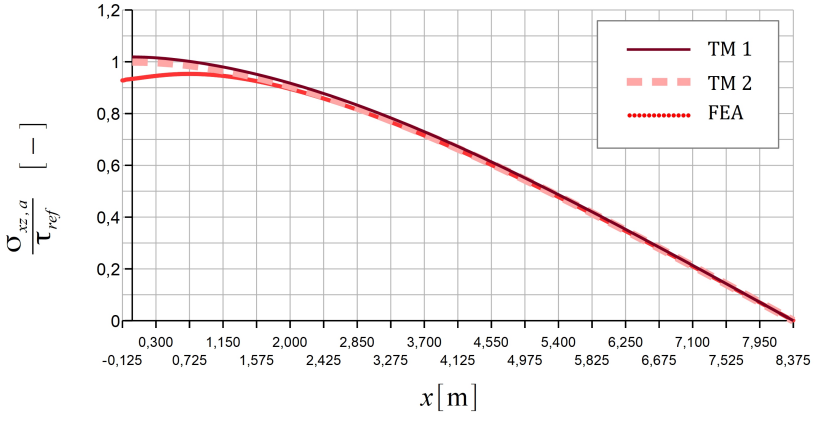

FIG. 11. Shear stress in the adhesive layer.

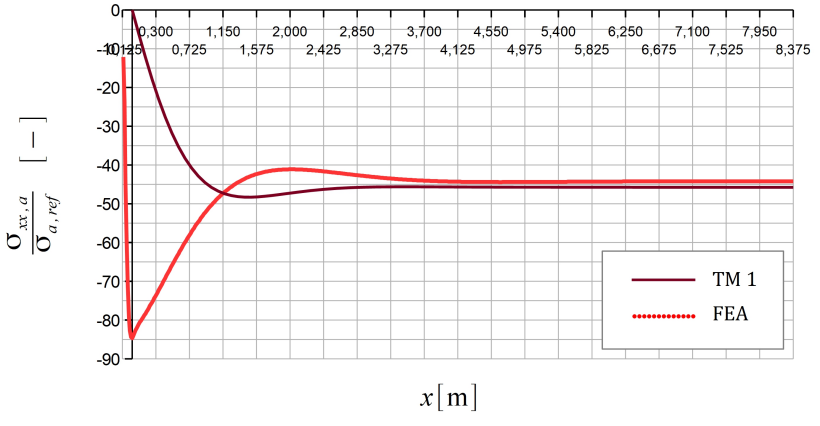

FIG. 12. Longitudinal normal stress in the adhesive layer.

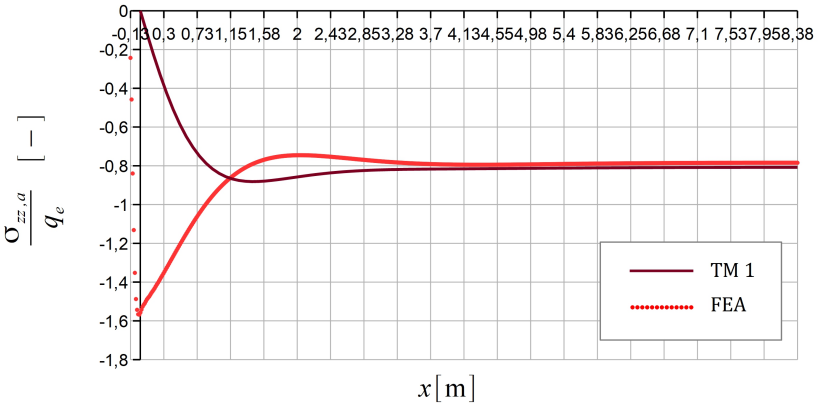

FIG. 13. Transverse normal (peel) stress in the adhesive layer.

It was observed that the through-the-width distribution of both longitudinal and transverse (peel) normal stress in the adhesive is not uniform – for this reason mean stresses were calculated and compared with theoretical predictions in Figs. 12 and 13.

4.2. Example No 2 – 4-point bending of a RC beam strengthened with a CFRP film

The second example deals with a reinforced-concrete beam strengthened with the use of the Sika©CarboDur© S512 CFRP strengthening film, attached to the bottom face of the beam with the use of Sika©PT stiff polyurethane. Geometry of the beam is shown in Fig. 14. The beam is simply supported – the span length is equal $L = 3\,\mathrm{m}$, overhangs are equal 10 cm. The beam is subject to four-point bending with two point forces $P = 20$ kN with loading points placed symmetrically on the beam at a distance 100 cm one from another. CFRP film is attached at a distance of 6 cm from the supported cross-section. Self-weight is disregarded as being negligibly small, compared to the external load.

The presence of the reinforcement was accounted for in the analytical model by the use of weighted geometric characteristics of the RC cross-section. The point load is accounted for by splitting the solution into two parts, each describing the deformation on one side of the loaded cross-section. Functions corresponding with the left part ($x \in (0; L/3)$) are denoted with (L) superscript, while those corresponding with the right part ($x \in (L/3; L/2)$) are denoted with (R). Since $\pi_{q1} = \pi_{q2} = 0$, the solution in each interval is given by the general solution of a homogeneous system, depending on 12 constants of integration. The 24 unknowns are determined from the linear system of algebraic equations given by the following boundary conditions and compatibility conditions:

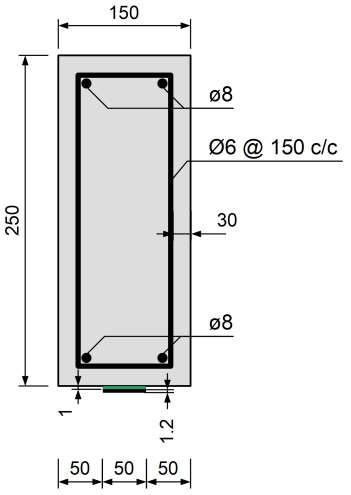

FIG. 14. Cross-section of an RC beam strengthened with a CFRP film.

(4.8)
$$\begin{array}{cc} \text{boundary conditions} & \text{boundary conditions} \\ \text{on supported end:} & \text{in the middle of the span:} \\ \begin{cases} N_1^{(L)}(0)=0, \\ N_2^{(L)}(0)=0, \\ M_1^{(L)}(0)=0, \\ M_2^{(L)}(0)=0, \\ w_2^{(L)}(0)=0, \\ \sigma_{xx,a}^{(L)}(0)=0, \end{cases} & \begin{cases} u_1^{(R)}(L/2)=0, \\ u_2^{(R)}(L/2)=0, \\ Q_1^{(R)}(L/2)=0, \\ Q_2^{(R)}(L/2)=0, \\ \phi_1^{(R)}(L/2)=0, \\ \phi_2^{(R)}(L/2)=0, \end{cases} \end{array}$$

(4.9)
$$\begin{array}{cc} \text{displacement compatibility:} & \text{force equilibrium:} \\ \begin{cases} u_1^{(L)}(L/3)=u_1^{(R)}(L/3), \\ u_2^{(L)}(L/3)=u_2^{(R)}(L/3), \\ \phi_1^{(L)}(L/3)=\phi_1^{(R)}(L/3), \\ \phi_2^{(L)}(L/3)=\phi_2^{(R)}(L/3), \\ w_1^{(L)}(L/3)=w_1^{(R)}(L/3), \\ w_2^{(L)}(L/3)=w_2^{(R)}(L/3), \end{cases} & \begin{cases} N_1^{(L)}(L/3)=N_1^{(R)}(L/3), \\ N_2^{(L)}(L/3)=N_2^{(R)}(L/3), \\ Q_1^{(L)}(L/3)=Q_1^{(R)}(L/3)+P, \\ Q_2^{(L)}(L/3)=Q_2^{(R)}(L/3), \\ M_1^{(L)}(L/3)=M_1^{(R)}(L/3), \\ M_2^{(L)}(L/3)=M_2^{(R)}(L/3). \end{cases} \end{array}$$

Linear elasticity is assumed in the numerical model and cracking of concrete is neglected. Reinforcement bars are modelled as truss elements embedded in the concrete beam. Full adhesion is assumed between the CFRP film and the adhesive layer. Since finer mesh was used for the adhesive and CFRP, compared to the RC beam, interface between adhesive and concrete was tied. The immovable support was modelled as a rigid body and the frictional contact was assumed between concrete and the support. Due to contact analysis, geometric non-linearity was accounted for in the numerical analysis, however its impact on

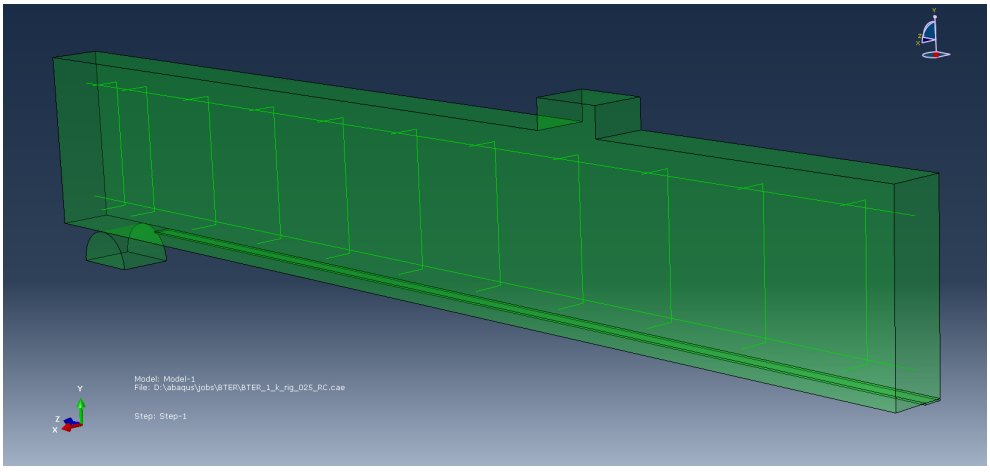

FIG. 15. Numerical model and RC beam strengthened with a CFRP film.

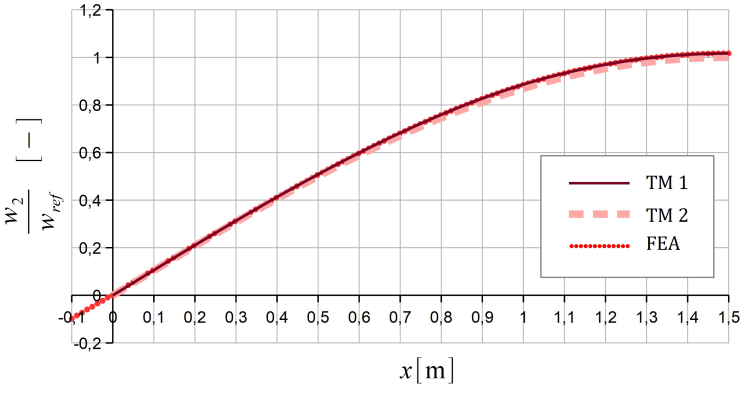

FIG. 16. Deflection of the bottom face of the RC beam.

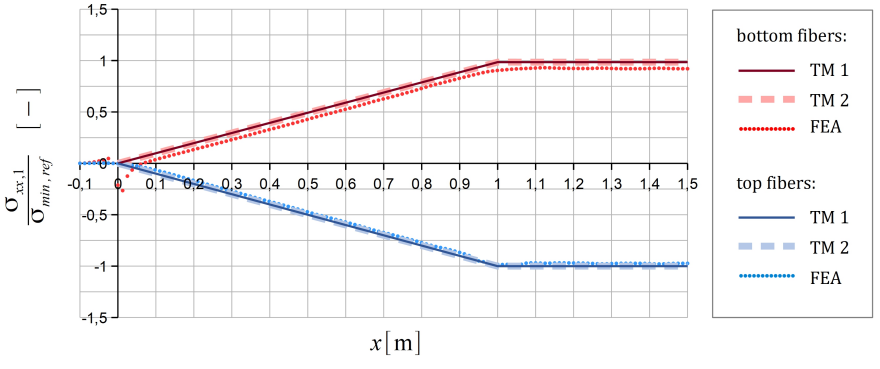

FIG. 17. Normal stress in top and bottom fibers of the RC beam.

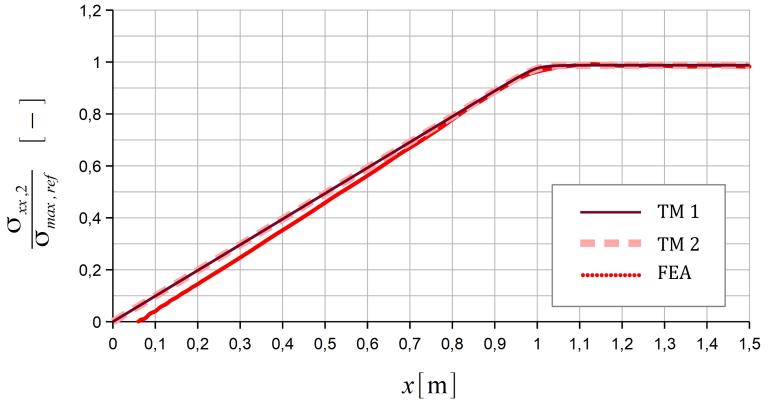

FIG. 18. Normal stress in the centroid of the CFRP film.

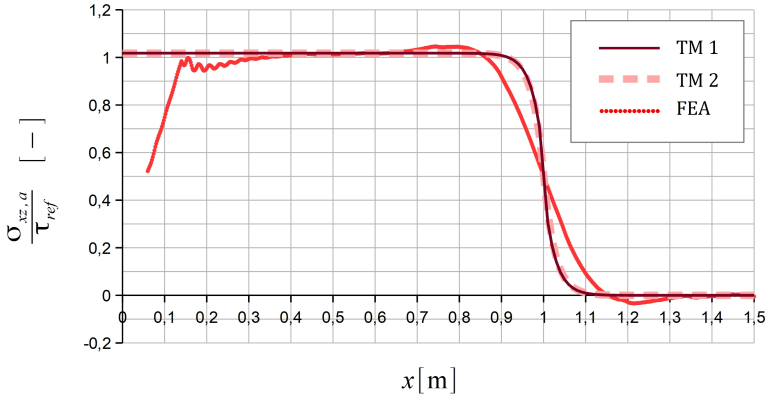

FIG. 19. Shear stress in the adhesive layer.

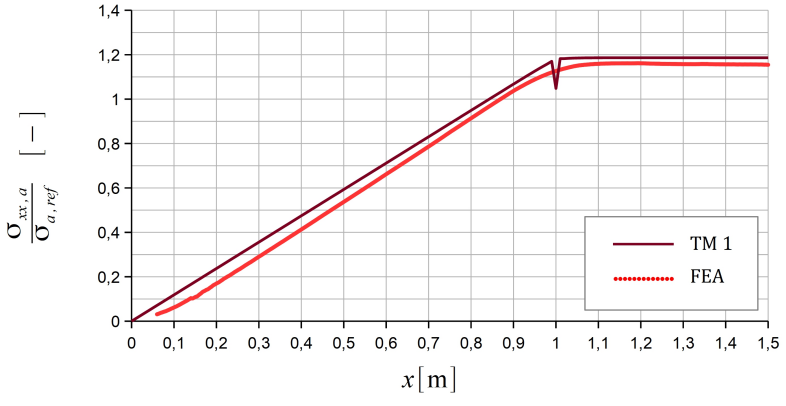

FIG. 20. Longitudinal normal stress in the adhesive layer.

the final results is negligible. The bottom face of the support is fixed. Symmetry conditions are prescribed so that only a quarter of the system may be modelled (Fig. 15). External load was applied in the form of enforced displacement of a steel plate pressing the beam through an elastomeric spacer.

Graphs presented in Figs. 16–20 show the relative deflection, edge normal stresses in the RC beam, average stress in CFRP film as well as longitudinal normal and shear stress in the adhesive layer. The reference values are calculated according to (4.1) and (4.4) with:

$$\alpha_k = \frac{23}{216}, \qquad M_R = \frac{PL}{3}, \qquad q_e = \frac{2P}{bl}.$$

The results of the FEA exhibit some irregularities in the distribution of stresses in the adhesive layer, which are caused most probably by significant mesh mismatch between two tied surfaces, namely the bottom face of the RC beam and much more finely meshed top face of the adhesive layer. The curves were regularized by plotting an average value over a neighborhood of each considered point. These smoothened curved are presented in Figs. 19 and 20.

It may be seen that compatibility conditions (4.9) ensure continuity of all generalized displacements as well as their derivatives except for the derivatives of deflection (which is different from an angle of rotation in the Timoshenko–Ehrenfest theory). This discontinuity makes also the distribution of $\frac{d\varepsilon_{zz,a}}{dx}$ discontinuous, what in turn affects the distribution of stresses $\sigma_{xx,a}$ and $\sigma_{zz,a}$. As a result the obtained peel stress distribution is unrealistic and for this reason it was not presented. The effect of discontinuity of derivatives of these stresses may be observed in Fig. 20. Analysis of additional examples indicates that such a disturbance is stronger for more stiff adhesive layers. In order to overcome this drawback of the presented theory, one may model any point load in the form of linear load distributed over a very short section of a beam.

5. Summary and conclusions

A theoretical model of a composite girder with an adhesive bondline was presented in the paper. The system of governing equations was derived from equations of equilibrium of cross-sectional forces after employing fundamental relations of the linear theory of elasticity and constitutive relations of the Timoshenko–Ehrenfest beam theory together with kinematic constraints on deformation of the adhesive layer. The obtained system of equations was transformed into a linear non-homogeneous system of the first order ordinary differential equations expressed in terms of the similarity numbers. The analytical solution was found with the use of the method of generalized eigenvectors. Analytical solutions were then validated numerically by comparison with solutions of

two distinct 3D problems, obtained with the use of the Finite Element Method. According to the obtained results following conclusions may be formulated:

- Accounting for shear deformation of beams (the Timoshenko–Ehrenfest theory) as well as for extensibility of the adhesive layer has minor impact on the results obtained from theoretical models. A relative difference between predictions of these two models, as regards displacements and stresses, is within ca. $0.5\% \div 7\%$. It indicates that disregarding the above mentioned issues in the TM 2 presented in [45, 46, 48] do not introduce a significant error. It may be of practical importance as this simplified model provides closed-form expressions for i.e. maximal deflection or maximal stresses [47, 48], as opposed to the refined TM 1, for which such expressions are impossible to derive due to their complexity. On the other hand, the TM 1 model presented in this research enables estimation of longitudinal normal stress in the adhesive, contrary to the simplified TM 2.
- Theoretical estimates of a maximal deflection are in good agreement with the results of FEA, with the relative error not exceeding 4%. The refined theoretical model TM 1 provides somewhat better prediction.
- Similarly the maximal shear stress in the adhesive is estimated well by both theoretical models, with a relative difference from the FEA results less than 5%. While the maximal value and overall distribution of shear stress in the adhesive are reproduced correctly, the true distribution is less uniform than the one predicted theoretically – this is due to the influence of boundary conditions in the neighborhood of the supported zone.
- Both longitudinal and transverse (peel) stresses in the adhesive in a beam subject to UDL are estimated correctly in the areas which are sufficiently distant from the supports. Close to the areas where kinematic boundary conditions are specified, theoretical estimates significantly underestimate the magnitude of stress.
- In case of beams loaded with point forces the proposed theory do not describe the distribution of peel stress correctly. Distribution of axial normal stress in adhesive is flawed by discontinuity of derivative of deflection, however, it may still provide a sufficiently accurate estimation.
- The relative error of theoretical estimates of normal stresses in edge fibers of adhesively bonded elements is within $0,5\% \div 26\%$. In most of cases TM 1 and TM 2 slightly overestimate the results of the FEA, providing safe estimates – the only deviation from this rule regards compressive stress in bottom fibers of an RC slab in a composite bridge deck, however, the greatest compressive stress occurs anyway in top fibers. It has already been observed that TM 2 provides safe estimates of normal stresses in the outermost material fibers [45–47]. Since discrepancies between the two considered models are relatively small, one should expect that this property

should also concern the presented TM 1 model – this should be, however, verified by a more extensive study.

- It is worth to notice that the simple composite Bernoulli–Euler theory utilizing weighted characteristics of a cross-section gives good approximation of normal stresses in edge fibers of the top and the bottom beam (the relative stresses are close to 1 in Figs. 9, 10, 17 and 18). It fails, however, in estimation of deflection of the beam and longitudinal normal stress in the adhesive layer (see Figs. 8, 12 and 20).

It may be stated that the presented theoretical model provides a useful tool for analysis of adhesively bonded composite girders. Its predictions are in fair agreement with the results of the detailed 3D Finite Element Analysis. Calculations may be performed by any numeric and/or symbolic computing environment – this research was carried out using free and open source software, namely wxMaxima 19.05.7 and GNU Octave 7.1.0. After rewriting all necessary formula, preparation of an executable script accounting for the assumed beam's load and support layout is far less time-consuming than elaboration of the FEM model. Such a script enables solving whole class of corresponding problems, unlike the FEM model which corresponds with a fixed geometry. Further research may focus on refining the obtained solutions in the areas where boundary effects become significant.

Acknowledgements

I would like to thank dr hab. inż. Dorota Jasińska, prof. PK from the Cracow University of Technology for her kind advices concerning the Finite Element Analysis.

References

1. L.F.M. da Silva, A. Öchsner, R.D. Adams [eds.], *Handbook of Adhesion Technology,* Springer, Cham, 2011.
2. H.M. Clearfield, D.K. McNamara, G.D. Davis, *Adherend Surface Preparation for Structural Adhesive Bonding*, in: L.-H. Lee [ed.], *Adhesive Bonding,* Springer Science+Bussiness Media New York, New York, 1991.
3. G. Viana, M. Costa, L.F.M. da Silva, M.D. Banea, *A review on the temperature and moisture degradation of adhesive joints*, Proceedings of the Institution of Mechanical Engineers, Part L: Journal of Materials: Design and Applications, **231**, 5, 488–501, 2017.
4. E.A.S. Marques, L.F.M. da Silva, M.D. Banea, R.J.C. Carbas, *Adhesive joints for low- and high-temperature Use: An overview*, The Journal of Adhesion, **91**, 7, 556–585, 2015.

5. C.B.G. BRITO, R.C.M. SALES, M.V. DONADON, *Effects of temperature and moisture on the fracture behaviour of composite adhesive joints*, International Journal of Adhesion and Adhesives, **100**, 102607, 2020.
6. P. GALVEZ, S. LOPEZ DE ARMENTIA, J. ABENOJAR, M.A. MARTINEZ, *Effect of moisture and temperature on thermal and mechanical properties of structural polyurethane adhesive joints*, Composite Structures, **247**, 112443, 2020.
7. F.C. AMORIM, J.M.L. REIS, J.F.B. SOUZA, H.S. DA COSTA MATTOS, *Investigation of UV exposure in adhesively bonded single lap joints*, Applied Adhesion Science, **6**, 1, 2018.
8. P.R. JAISWAL, N.S. HIRULKAR, P.N.B. REIS, L. PAPADAKIS, S.N. KHAN, *Effect of cyclic solar (UV) radiation and temperature on mechanical performance of single lap adhesive joint*, 2017 ICICICT Conference, 182–189, 2017.
9. G. DOYLE, R.A. PETHRICK, *Environmental effects on the ageing of epoxy adhesive joints*, International Journal of Adhesion and Adhesives, **29**, 1, 77–90, 2009.
10. A. RIDER, E. YEO, *The Chemical Resistance of Epoxy Adhesive Joints Exposed to Aviation Fuel and its Additives*, Technical Report DSTO-TR-1650 of the Defence Science and Technology Organisation, 2005.
11. H.R. GUALBERTO, F. DO CARMO AMORIM, H.R.M. COSTA, *A review of the relationship between design factors and environmental agents regarding adhesive bonded joints*, Journal of the Brazilian Society of Mechechanical Sciences and Engineering, **43**, 8, 1–19, 2021.
12. R.A. PETHRICK, *Design and ageing of adhesives for structural adhesive bonding – A review*, Proceedings of the Institution of Mechanical Engineers, Part L: Journal of Materials: Design and Applications, **229**, 5, 349–379, 2015.
13. V.A. SILVESTRU, G. KOLANY, B. FREYTAG, J. SCHNEIDER, O. ENGLHARDT, *Adhesively bonded glass-metal façade elements with composite structural behaviour under in-plane and out-of-plane loading*, Engineering Structures, **200**, 109692, 2019.
14. M. BUES, C. SCHULER, M. ALBEIZ, T. UMMENHOFER, H. FRICKE, T. VALLÉE, *Load bearing and failure behaviour of adhesively bonded glass-metal joints in façade structures*, The Journal of Adhesion, **95**, 5-7, 653–674, 2019.
15. K.U. SCHOBER, A.M. HARTE, R. KLIGER, R. JOCKWER, Q. XU, J.F. CHEN, *FRP reinforcement of timber structures*, Construction and Building Materials, **97**, 106–118, 2015.
16. S.A. BABATUNDE, *Review of strengthening techniques for masonry using fiber reinforced polymers*, Composite Structures, **161**, 246–255, 2017.
17. A. KWIECIEŃ, G. DE FELICE, D.V. OLIVEIRA, B. ZAJĄC, A. BELLINI, S. DE SANTIS, B. GHIASSI, G.P. LIGNOLA, P.B. LOURENÇO, C. MAZZOTTI, A. PROTA, *Repair of composite-to-masonry bond using flexible matrix*, Materials and Structures, **49**, 7, 2563–2580, 2016.
18. A. KWIECIEŃ, P. KUBOŃ, *Dynamic analysis of damaged masonry building repaired with the flexible joint method*, Archives of Civil Engineering, **58**, 1, 39–55, 2012.
19. Y.H. MUGAHED AMRAN, R. ALYOUSEF, R.S.M. RASHID, H. ALABDULJABBAR, C.C. HUNG, *Properties and applications of FRP in strengthening RC structures: A review*, Structures, **16**, 208–238, 2018.
20. L.A. MODESTI, A.S. DE VARGAS, E.L. SCHNEIDER, *Repairing concrete with epoxy adhesives*, International Journal of Adhesion and Adhesives, **101**, 102645, 2020.

21. K. Rashid, M. Ahmad, T. Ueda, J. Deng, K. Aslam, I. Nazir, M. Azam Sarwar, *Experimental investigation of the bond strength between new to old concrete using different adhesive layers*, Construction and Building Materials, **249**, 118798, 2020.

22. J.G. Broughton, A.R. Hutchinson, *Adhesive systems for structural connections in timber*, International Journal of Adhesion and Adhesives, **21**, 3, 177–186, 2001.

23. G. Tłustochowicz, E. Serrano, R. Steiger, *State-of-the-art review on timber connections with glued-in steel rods*, Materials and Structures, **44**, 5, 997–1020, 2011.

24. J. Custódio, J. Broughton, H. Cruz, *A review of factors influencing the durability of structural bonded timber joints*, International Journal of Adhesion and Adhesives, **29**, 2, 173–185, 2009.

25. M. Heshmati, R. Haghani, M. Al-Emrani, *Environmental durability of adhesively bonded FRP/steel joints in civil engineering applications: State of the art*, Composites Part B: Engineering, **81**, 259–275, 2015.

26. P. Kumar, A. Patnaik, S. Chaudhary, *A review on application of structural adhesives in concrete and steel–concrete composite and factors influencing the performance of composite connections*, International Journal of Adhesion and Adhesives, **77**, 1–14, 2017.

27. Y. Shu, X. Qiang, X. Jiang, Y. Xiao, H. Dong, *Long-term performance of single-lap joints: Review, challenges and prospects in civil engineering*, Engineering Reports, 1–22, 2023.

28. J. Kanócz, V. Bajzecerová, *Timber – concrete composite elements with various composite connections. Part 3: Adhesive connection*, Wood Research, **60**, 6, 939–952, 2015.

29. S.-Y. Baek, Y.-J. Song, S.-H. Yu, D.-H. Kim, S.-I. Hong, *Bending of CLT-concrete slabs*, BioResources, **16**, 4, 8227–8238, 2021.

30. L. de Waal, D. Fernando, V.T. Nguyen, R. Cork, J. Foote, *FRP strengthening of 60 year old pre-stressed concrete bridge deck units*, Engineering Structures, **143**, 346–357, 2017.

31. A. Zhou, T. Keller, *Joining techniques for fiber reinforced polymer composite bridge deck systems*, Composite Structures, **69**, 3, 336–345, 2005.

32. T. Keller, H. Gürtler, *Composite action and adhesive bond between fiber-reinforced polymer bridge decks and main girders*, Journal of Composites for Construction, **9**, 4, 360–368, 2005.

33. O. Volkersen, *Die Nietkraftverteilung in zugbeanspruchten Nietverbindungen mit konstanten Laschenquerschnitten*, Luftfahrtforschung, **15**, 41–47, 1938.

34. N.A. de Bruyne, *The strength of glued joints*, Aircraft Engineering, **16**, 115–118, 1944.

35. A. Kwiecień, *Shear bond of composites-to-brick applied with highly deformable, in relation to resin epoxy, interface materials*, Materials and Structures, **47**, 12, 2005–2020, 2014.

36. A. Kwiecień, P. Krajewski, Ł. Hojdys, M. Tekieli, M. Słoński, *Flexible adhesive in composite-to-brick strengthening-experimental and numerical study*, Polymers, **10**, 4, 1–23, 2018.

37. J.R. Cruz, J. Sena-Cruz, M. Rezazadeh, S. Seręga, E. Pereira, A. Kwiecień, B. Zając, *Bond behaviour of NSM CFRP laminate strip systems in concrete using stiff and flexible adhesives*, Composite Structures, **245**, 1–18, 2020.

38. W. Derkowski, A. Kwiecień, B. Zając, *CFRP strengthening of bent RC elements using stiff and flexible adhesives*, Technical Transactions, **1-B/2013**, 37–52, 2013.

39. J.R. CRUZ, S. SAREĘGA, J. SENA-CRUZ, E. PEREIRA, A. KWIECIEŃ, B. ZAJĄC, *Flexural behaviour of NSM CFRP laminate strip systems in concrete using stiff and flexible adhesives*, Composites Part B: Engineering, **195**, 108042, 2020.

40. S. ABRATE, M. DI SCIUVA, *Multilayer Models for Composite and Sandwich Structures*, in: P.W.R. BEAUMONT, C.H. ZWEBEN [eds.], Comprehensive Composite Materials II, Elsevier, 2018.

41. D. LI, *Layerwise Theories of laminated composite structures and their applications: a review*, Archives of Computational Methods in Engineering, **28**, 2, 577–600, 2021.

42. A. TESSLER, M. DI SCIUVA, *Refinement of Timoshenko Beam Theory for Composite and Sandwich Beams Using Zigzag Kinematics*, NASA Technical Publication 2007-215086, 2007.

43. S. ABRATE, M. DI SCIUVA, *Equivalent single layer theories for composite and sandwich structures: A review*, Composite Structures, **179**, 482–494, 2017.

44. G. SCHICKHOFER, *Monographic Series TU Graz: Starrer und nachgiebiger Verbund bei geschichteten, flächenhaften Holzstrukturen*, Verlag der Technischen Universität Graz, Graz, 2013.

45. P. SZEPTYŃSKI, *Comparison and experimental verification of simplified one-dimensional linear elastic models of multilayer sandwich beams*, Composite Structures, **241**, 112088, 2020.

46. P. SZEPTYŃSKI, *Closed-form analytical solution to the problem of bending of a multilayer composite beam – derivation and verification*, Composite Structures, **291**, 115611, 2022.

47. P. SZEPTYŃSKI, J. POCHOPIEŃ, D. JASIŃSKA, A. KWIECIEŃ, *The influence of the flexibility of a polymeric adhesive layer on the mechanical response of a composite reinforced concrete slab and a reinforced concrete beam girder*, Polymers, **16**, 444, 2024.

48. P. SZEPTYŃSKI, *Analytical modelling of thin shear plywoodquasi-static sheared (Analityczne modelowanie cienkich sklein ścinanych quasi-statycznie*), Cracow University of Technology Publishing House, Kraków, 2023 [in Polish].

49. P. SZEPTYŃSKI, D. JASIŃSKA, L. MIKULSKI, *Analytical modelling and shape optimization of composite girder with adhesive bondline*, Journal of Theoretical and Applied Mechanics, **62**, 1, 129–142, 2024.

50. M. GOLAND, E. REISSNER, *The stresses in cemented joints*, Journal of Applied Mechanics, **11**, A17–A27, 1944.

51. F. DELALE, F. ERDOGAN, M.N. AYDINOGLU, *Stresses in Adhesively Bonded Joints: a Closed-Form Solution*, NASA Contractor Report 165638, 1980.

52. C. YANG, S.S. PANG, *Stress-strain analysis of single-lap composite joints under tension*, Journal of Engineering Materials and Technology, Transactions of the ASME, **118**, 2, 247–255, 1996.

53. D.J. ALLMAN, *A theory for elastic stresses in adhesive bonded lap joints*, Quarterly Journal of Mechanics and Applied Mathematics, **30**, 4, 415–436, 1977.

54. S.P. TIMOSHENKO, J.M. GERE, *Mechanics of Materials*, 2nd ed., PWS-KENT Publishing Company, Boston, 1984.

55. D.I. ZHURAVSKY, *Sur la résistance d'un corps prismatique et d'une pièce composée en bois ou en tôle de fer à une force perpendiculaire à leur longueur*, Mémoires Annales des Ponts et Chaussées, **2**, 328–351, 1856.

56. F. GRUTTMANN, W. WAGNER, *Shear correction factors in Timoshenko's beam theory for arbitrary shaped cross-sections*, Computational Mechanics, **27**, 199–207, 2001.

57. I.U. OJALVO, H.L. EIDINOFF, *Bond thickness effects upon stresses in single-lap adhesive joints*, AIAA Journal, **16**, 3, 204–211, 1978.

58. M.Y. TSAI, D.W. OPLINGER, J. MORTON, *Improved theoretical solutions for adhesive lap joints*, International Journal of Solids and Structures, **35**, 12, 1163–1185, 1998.

59. D.A. BIGWOOD, A.D. CROCOMBE, *Elastic analysis and engineering design formulae for bonded joints*, International Journals of Adhesion and Adhesives, **9**, 4, 229–242, 1989.

60. W.J. RENTON, J.R. VINSON, *Analysis of adhesively bonded joints between panels of composite materials*, Journal of Applied Mechanics, **44**, 1, 101–106, 1977.

61. L.J. HART-SMITH, *Adhesive Bonded Single-lap Joints*, NASA Report: CR-112236, 1973.

62. P.A. COOPER, J.W. SAWYER, *Critical Examination of Stresses in an Elastic Single Lap Joint*, NASA Technical Paper 1507, 1979.

63. University of Oslo, Lecture notes on generalized eigenvectors for systems with repeated eigenvalues, course differential equations and optimal control theory, 1–8, 2011.

64. P. SZEPTYŃSKI, *Corrigendum to "Closed-form analytical solution to the problem of bending of a multilayer composite beam – Derivation and verification"*, Composite Structures, **299**, 116028, 2022.

65. I.N. BRONSHTEIN, K.A. SEMENDYAYEV, *Handbook of Mathematics, 4^{th} Edition*, Springer-Verlag, Berlin, 2004.

66. European Committee for Standardisation, EN 1992-1-1:2008, Eurocode 2: Design of concrete structures, 2008.

67. European Committee for Standardisation, EN 1993-1-1 – Eurocode 3: Design of steel structures – Part 1-1: General rules and rules for buildings, 2006.

68. Sika Corporation, PRODUCT DATA SHEET Sika©CarboDur©S (Version 05.03), 2024.

69. E. HARA, T. YOKOZEKI, H. HATTA, Y. IWAHORI, T. ISHIKAWA, *CFRP laminate out-of-plane tensile modulus determined by direct loading*, Composites Part A: Applied Science and Manufacturing, **41**, 10, 1538–1544, 2010.

70. J. KARPIESIUK, *Young's modulus and Poisson's ratio of polyurethane adhesive in lightweight floor system*, Modern Approaches on Material Science, **2**, 3, 251–255, 2020.

71. D. TSUKINOVSKY, E. ZARETSKY, I. RUTKEVICH, *Material behavior in plane polyurethane-polyurethane impact with velocities from 10 to 400 m/sec*, Journal De Physique IV, **7**, C3, C3-335–C3-339, 1997.

Received March 11, 2024; revised version May 6, 2024.
Published online May 21, 2024.